

Polytechnic University of Turin



DEPARTMENT OF CONTROL AND COMPUTER ENGINEERING (DAUIN)

MASTER OF SCIENCE IN MECHATRONIC ENGINEERING

MASTER DEGREE THESIS

**Model Based Design of Field Oriented Control of Brushless
Motor for Automotive Fuel Pump**

Supervisor:
Prof. Massimo Violante

Candidate:
Mahdi Kazemi

September 2018

Abstract:

In this master thesis control of automotive fuel pump has studied. Today, automotive fuel system is an important section of automotive that need improvement because of decreasing air pollution and also better way to decrease energy consumption. And fuel pump is one of important part of fuel system. With a sufficient fuel delivery, it is possible to remove the return fuel line to the fuel tank of automotive. For this purpose a good and sufficient fuel pump is needed.

In the first chapter different fuel pump types are discussed. Then electric motor that is the main part of fuel pump described, after that best motor for fuel pump is selected. The main part of control that described in the thesis is the speed control brushless motor that with respect to it the fuel that pumped is controlled. Also, the other parts of motor control like torque is considered that they are described in detail in the following paragraphs. Fluid dynamic of the pump and which pump is a good option is also discussed and regenerative pump is selected and it used in simulation.

Field oriented control (FOC) is one the best motor control that nowadays, it is also implemented to brushless motors. With FOC the motor the torque ripple is decrease, and current and speed control is also implement in FOC. One of control term that it is used is maximum torque per ampere (MTPA), with MTPA torque control is added to the control and also the quadrature current is created. Then Field oriented control is used for flux control of the motor. With field oriented control, it possible to increase speed when maximum back-emf is reached, it term of operation is like that it decrease the quadrature current that cause flux reduction and it will not allow the increase of the back-emf.

In mechanical part of pump that it is casing and fuel pump, the regenerative pump is used. Regenerative pump is one the best pump for high pressure delivery of the fuel to the engine. It mathematical modelling and term of operation is described. And also the fuel characteristic that is one of important part of fuel pressure is also shown.

For simulation of the fuel pump (motor and hydraulic) Matlab, Simulink and Simscape are used. Then the result of simulation if shown in chapter 5. The simulation result shown the motor operation in reference speed change, battery state of charge change, field weakening. Also, the motor operation effect on fuel pressure and flow rate. And some safety operation that needed in modern electric fuel pump is also discussed.

The torque of the pump that it is according to the speed of the motor and the load of the pump is calculated and it is connected to the motor, that it cause direct effect of torque of electrical motor performance. The pressure simulation for the desired reference values of pressure is done. Also the voltage change effect, motor speed in pressure of the pump. The simulation result are shown in chapter six.

Acknowledgement:

I would like to express my very appreciation to my supervisor prof. Massimo Violante, for suggesting this project and for all of his support, patience and dedication offered his time to help me to finishing this thesis.

I would also like to express my deep gratitude to my family for their support and encouragement throughout my study.

Table of Contents

1. Introduction	1
1.1 Purpose	2
1.2 Model based design (MBD)	2
1.3 Introduction to Fuel pump	2
1.3.1 Mechanical fuel pump	4
1.3.2 Electrical fuel pump	4
1.4 Electrical motor	5
2. fuel pump	8
2.1 Automotive fuel pump types	8
2.2 Pump types	9
2.2.1 Positive displacement pump	9
2.2.2 Variable displacement pump	9
2.2.3 Velocity pump or rotor-dynamic pump	9
2.3 Regenerative turbine pump	10
2.4 Mathematical Model of regenerative turbine pump	12
2.5 Fuel	14
2.6 Mathematical modeling in Simscape	15
3 Brushless Motor and Mathematical Modeling	17
3.1 Brushless (BLDC) motor operation	17
3.1.1 Inverter	18
3.1.1.1 Snubber circuit	19
3.1.2 Control	19
3.2 Fundamental of BLDC motor	20
3.2.1 Stator	20
3.2.2 Rotor	21
3.2.3 Sensor	22
3.2.4 BEMF (back electromotive force)	22
3.3 Mathematical model	22
4 Field Oriented Control	27
4.1 Vector reference frame	27
4.1.1 Clark Transformation	28
4.1.2 Inverse Clark transformation	29
4.1.3 Park Transformation	29
4.2 Space vector modulation	30
4.3 Current Control	31
4.3.2 Tuning the i_{sd} PI controller	37
4.3 Speed control	41

4.4 Anti-windup for Current loop controller -----	43
4.5 Maximum Torque per Ampere (MTPA) -----	44
4.6 Field Weakening -----	46
5 Algorithm for Hydraulic Control -----	49
5.1 Pressure control -----	49
5.2 Fuel Pressure -----	50
5.4 Battery -----	51
5.5 Safety function -----	52
5.6 Control unit -----	53
6 Evaluation of Simulation Result -----	54
6.1 Electrical motor general characteristic -----	54
6.2 Hydraulic characteristic -----	57
6.3 Battery SOC effect -----	59
7 Conclusion -----	62
Reference -----	64
Appendix -----	66

Abbreviation:

ECU	Electronic control unit
AC	Alternating current
DC	Direct current
IM	Induction motor
SM	Synchronous motor
BLPMM	Brushless permanent magnet motor
BLDC	Brushless DC
PMSM	Permanent magnet synchronous motor
BEMF	Back electromotive force
FOC	Field oriented control
SVPWM	Space vector modulation
SPWM	Sinusoidal pulse with modulation
rpm	Rotation per minute
Gm	Gain margin
PM	Phase margin
SOC	State of charge
MBD	Model based design
MIL	Model in the loop
SIL	Software in the loop
PIL	Processor in the loop
HIL	Hardware in the loop
RMF	Rotating magnetic field
DTC	Direct torque control

Introduction

Automobiles for starting their operations need energy source. This energy source can be supplied by different kind of fuel. In combustion engine and hybrid¹ cars, the fuel system is an important part of the automotive. For making a cost effective fuel system and improvement according to standards, the improvement of the fuel system is a one of the main part of automotive. One example of fuel system improvement is removing of return pipeline of the fuel for reducing the energy loss due to the extra fuel that entering the system in internal combustion engine vehicles.

As it is mentioned above, the amount of the fuel that is delivered to the engine must have been controlled for reducing the energy losses and match the standards (for example one solution of reducing CO₂ exhaust is sufficient fuel supply) [3]. Many parts of fuel system have include to achieve this improvement. The automotive fuel system in general include the following parts; also it is shown in the figure 1.1.

1. Fuel tank: the fuel is stored in the fuel tank, and it is safe container for flammable fuel.
2. Filter: A fuel filter is a filter in the fuel line that screens out dirt and dust particles from the fuel, normally made into cartridges containing a filter paper. They are found in most internal combustion engines [4].
3. ECU: Electronic control unit (ECU) is the control part of modern automobile. It control the precise amount of fuel delivered to the engine [3] with respect to engine performance. For example controlling solenoids (injectors), pump and etc.
4. Fuel line: it carry fuel in system and its type depend to location line in the fuel system.
5. Fuel Pump: fuel pump supply the fuel from the fuel tank to the system, and it is modelled and is simulated in depth in this thesis.
6. Fuel injection: in general the fuel injection supply the fuel to the combustion engine. In internal combustion engine also doing the mixing of fuel with air.

¹ Hybrid car use more than one resource; for example electric and fuel as alternative of supply.

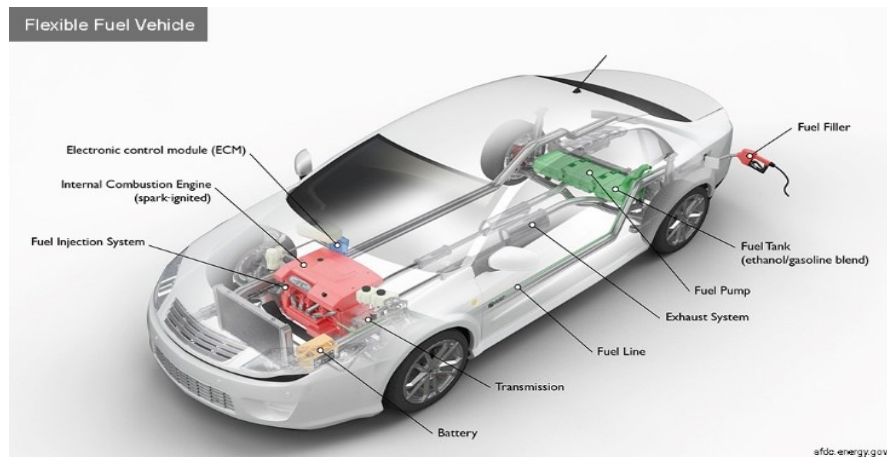


Figure 1.1 Automobile Fuel system

1.1 Purpose

Fuel pump is one of the essential part of the automotive fuel system. This thesis focus on fuel pressure control that the pump have to deliver it to engine. To achieve this goal the hydraulic flow rate and pressure control is needed. For a great hydraulic control a good type of pump is needed to deliver the desired amount of fuel to the engine. The hydraulic control and motor control are discussed in this thesis in order to achieve a good result. To achieve the result modeling and simulation of the pump are needed. Here, in this thesis Matlab and Simulink are used for simulation and implementation of controlling of electrical motor and hydraulic.

1.2 Model based design (MBD)

Nowadays, the computing power of the microprocessors are increasing. Also, the complexity of vehicles are increasing day-by-day that it need more complex and higher computation possibility. By increasing the complexity writing programming language codes manually is almost impossible due to the difficulties and it take a lot of time for designing. And as it is described, due to the existence of powerful processors MBD is a good method for designing and implementation of control algorithms.

In figure 1.2, MBD workflow is shown. The beginning part of MBD is to design an control algorithm and its environmental model. To implement a control algorithm there are software's like Simulink that give this possibility to create mathematical modelling. In order to make easier modeling some companies start to make software's with physical components in order to decrease modeling time, for example Modelica language and Simscape are such model and software's. After designing the model of control and plant, it is possible to simulate the model, and also to create codes and then implement it to the ECU, simulation methods of MBD are described in detail in the following paragraphs.

The most useful algorithm for designing and implementation of MBD in automotive part is the V-model method that it is shown in figure 1.3. The main concept of V-model is the same procedure that is shown in figure 1.2, but with a good scheduling that it is used almost in every MBD of automotive companies.

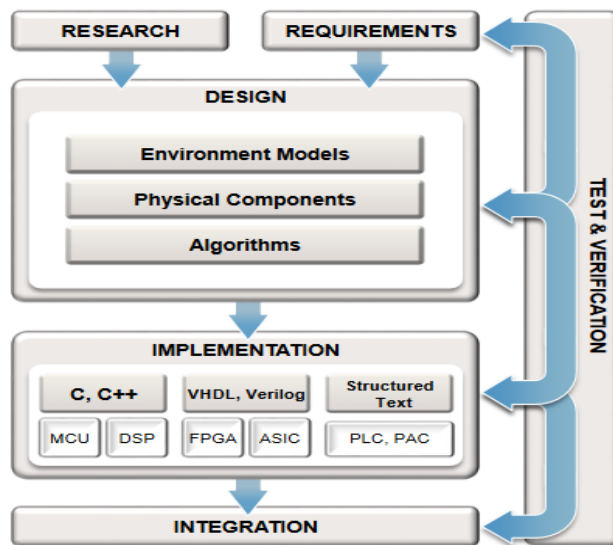


Figure 1.3 Model based design workflow

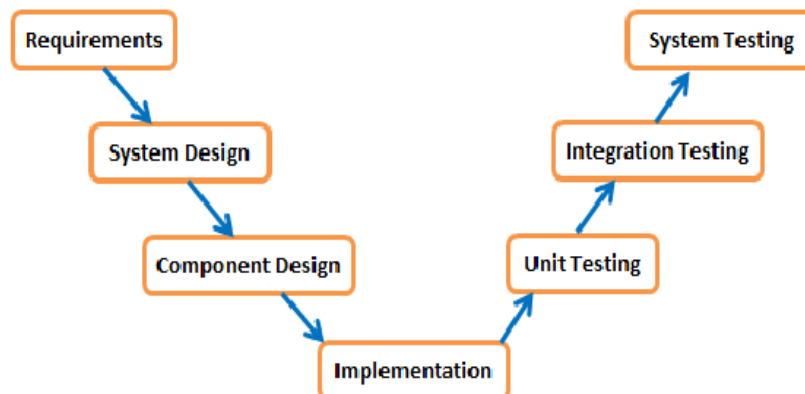


Figure 1.2 V-Model

MBD include four parts that they are Model-in-the-Loop (MIL), Software-in-the-Loop (SIL), Processor-in-the-loop (PIL) and Hardware-in-the-Loop (HIL). These steps are done to check each step in order if there is any fault at the specific step, correct it at that step that cause time and cost saving.

MIL is the first step of MBD for designing a control for specific plant. It include modelling of control part and plant for running. The control algorithm and the plant are designed by mathematical and physical component in specific software and then the simulation will done in order to verify the control algorithm that it is work properly or no. If it is not work properly edit the control algorithm and again the simulation will done in order to earn the desired result. In this thesis, MIL MBD is done in Matlab/Simulink software's in order to earn the desired control and result.

SIL is a step forward of the MIL. After creation of MIL, it is possible to execute the desired codes, like C language code with specific software's like TargetLink. Then, the code is replaced with the control algorithm model in order to know that the desired code is working the same as the MIL.

In PIL part, the control algorithm code is implemented to the desired control board and the plant model is available in the software, then by using real time simulation the control algorithm that is implemented to the control board is tested in order to see that the generated code work properly with the plant model.

HIL is the last step of MBD. In this stage, the plant hardware model is placed in the loop, in order to check that the simulation is also working great also with plant simulator. HIL is done when the plant is not available and also other benefit is that when the control have fault it is not damage the plant because it is the plant simulator. All four steps are shown in figure 1.4.

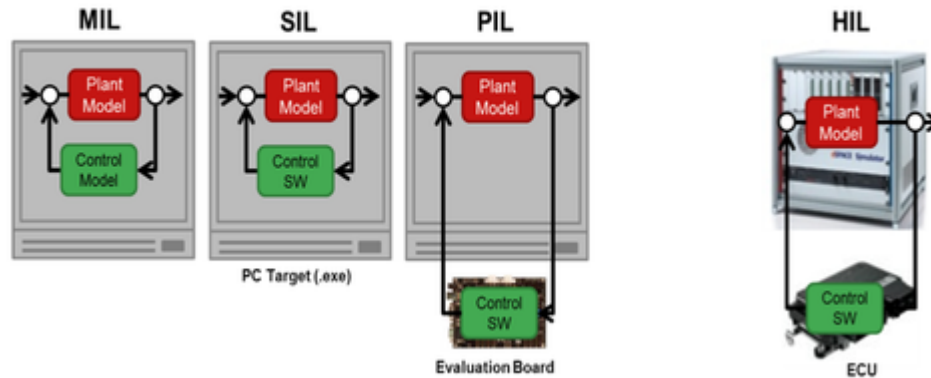


Figure 1.4 Four steps of MBD

1.3 Introduction to Fuel pump

Fuel pump supply fuel to engine and it is one of essential part of combustion engine. The main function of fuel pump is fuel supplement with the desired amount and pressure. In general two types of the fuel pumps have been used in vehicle fuel system that they are mechanical fuel pump and electrical fuel pump. They are described in the following.

1.3.1 Mechanical fuel pump

Mechanical fuel pumps are used mostly in carbureted vehicles to transfer the fuel to the carburetor. Fuel pumps on carbureted engines are usually mounted on the side of the engine block or cylinder head and operated by an eccentric on the engine's camshaft. The rocker arm of the pump rests against the camshaft eccentric, and as the camshaft rotates, it actuates the rocker arm [5]. Mechanical fuel pumps are usually made of flexible diaphragm and by movement of the diaphragm by rocker arm the pressure is processed in the pump. Mechanical fuel pump supply low pressure flow of fuel to carburetor. With development of automotive system, carburetor is replaced by the injection system that need more pressure of fuel supply as compare to carburetor that mechanical pump is not a good option for low pressure. Others disadvantage of mechanical pump are efficiency, leakage due to the usage of diaphragm and fuel heat increase due to the installation on engine.

1.3.2 Electrical fuel pump

Electrical pump convert electrical energy to hydraulic energy. In modern car that the fuel transfer is controlled with ECU, control of pump is also an important task. Nowadays, the pumps that they are controlled with solid state technology cause easy and efficient control, long life and etc.

It is more flexible with safety standards, for example cars with electronic fuel injection have an electronic control unit (ECU) and this may be programmed with safety logic that will shut down the electric fuel pump, even if the engine is running [4]. And these are the reasons that mechanical fuel pumps have been replaced with electrical fuel pump. The main part of electrical fuel pump control is electrical motor. Electrical motor control is the essential part in electrical pump control.

1.4 Electrical motor

Electrical Pump produce hydraulic energy by rotation of electrical motor that is installed inside the pump. There are many types of electrical motors with different specification and characteristic. Electrical motors generally divide into two groups: alternating current (AC) and direct current (DC).

AC motor is derived to move by alternating current. AC motors mainly are two type: induction motor (IM) and Synchronous motor (SM). In IM the driving current pass through stator coils, the current in stator coils create rotating magnetic field (RMF), because of rotating magnetic field in stator the electromotive force (EMF) create in the rotor wiring; the two field interact together and push rotor to rotate around and create mechanical rotational energy. The motor is called induction motor because the electricity is induced in rotor by electromagnetic induction. There is slip in IM, the rotor rotate in lower speed than stator RMF and this cause producing EMF in the rotor. Because of slip speed of IM is less than frequency of driving current. Synchronous motor (SM) is similar to IM; the difference are that speed of SM is synchronous to frequency of supply and the field is produce by permanent magnet or dc current. The main disadvantage of IM and SM are speed control of them in variable speed requirement [6].

DC motor have been popular due to their operating characteristic, their linear and stable speed-torque control [7]. DC motor have simple operation principle that can derive directly by DC voltage. Mechanical commutation are used for energizing rotating rotor coils. DC motors are cheaper and easy to control. But is has some disadvantage due to the usage of brushes for commutation, that it need maintenance and low life duration. Also due to the spark creation that create by commutation, also it is not a safe option to use it in flammable locations.

To overcome the disadvantage of DC motor brushless permanent magnet motor (BLPMM) are used. BLPMM are using electronics commutator for commutation, and rotor is made of permanent magnet. BLPMM is divided to two parts: brushless DC (BLDC) and permanent magnet synchronous (PMM). BLPMM is the improvement model of DC and AC motors. BLPMM use DC power supply for inverter and then inverter supply AC power to the motor. In some topic BLPMM are part of AC motor in some other are part DC motor and in rest is categorized in a separate branch. BLPMM energy efficiency are up to 97 percent [8], and also the size of their size is smaller than IM.

BLDC motor as mentioned above is brushless motor that increase life of the motor and remove maintenance need due to brushes that it was in brushed DC motor. BLDC motor rotor is made of permanent magnet; and the current supply by the inverter to stator. The inverter supply current with respect to rotor position that it is provided by Hall Effect sensors or by the estimation procedure. In BLDC motor inverter supply to stator is square waveform that it is pulse width change to provide the desired speed of the motor. BLDC are especially interesting for high speed application and applications where a continuous rotation is needed, also it cheaper as compare to interior PMSM [8, 9].

Motor type	DC motor	Induction motor	PM motor	Switched reluctance motor
Performance index				
Power density	Low	Intermediate	High	Very high
Peak efficiency (%)	<90	90–95	95–97	<90
Load efficiency (%)	80–87	90–92	85–97	78–86
Controllability	Simple	Complex	Hard for field-weakening	Complex
Reliability	Normal	Good	Excellent	Good
Heat dissipation	Bad	Bad	Good	Good
Size & weight	Big, Heavy	Normal, Normal	Small, Light	Small, Light
High-speed performance	Poor	Excellent	Good	Excellent
Construction	Slightly worse	Better	Slightly better	Excellent
Cost of motor (\$/kW)	10	8–10	10–15	6–10
Cost of controller	Low	High	High	Normal
Combination property	Slightly worse	Normal	Excellent	Better

Table 1.1 Motors Performance

PMSM work almost similar to BLDC motor; its difference with BLDC motor is inverter supply current to motor that it is sinusoidal waveform. PMSM machines are known to be the most expensive option but as the minimal configuration already requires position feedback they are ideally suited for accurate positioning [8]. BLPMM have better characteristic as compare with other electric motors that are frequently use in electric vehicle, it is shown in figure 1.5 and table 1.1 [10].

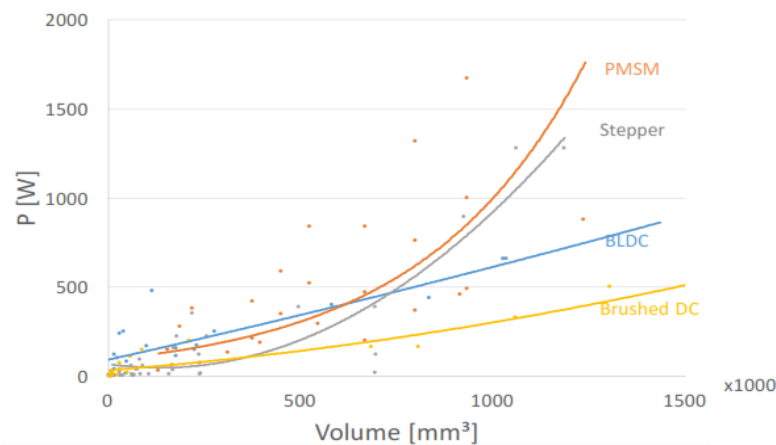


Figure 1.5 Motors operation with respect to power vs. its volume

A research were done in Gehnt university in Belgium [8] for speed versus power and power versus volume for compression of BLDC, PMSM result earned that it is showed in figure 2. As it is seen, acceleration of BLDC with respect to PMSM is higher. But the PMSM almost have constant power with respect to rotational speed. Also as shown in figure 1.5, with power increase also volume increase, for higher power interior PMSM pump has more volume. But in lower power BLDC motor has better performance.

Automotive fuel pump operate in low power range. According to performance of motors, BLPMM are good option for automotive fuel pump because of higher efficiency, lower weight and lower cost and better performance. Also in automobile electrical energy is supplied to pump is DC, thus a motor with DC derivable is better choice to fit to the electrical energy of battery. BLDC motor are cheaper and in some control is easier to control than PMSM [9], but a torque ripple is a little bit more than PMSM. Also some method are improvement for decrease of torque ripple in BLDC motor. Brushless dc motor drives provide higher output power density than of sinusoidal machines for the same rated current and BEMF peak values [12]. In this thesis with respect to above information the BLPMM may be the best option for automotive electrical fuel pump. BLDC name is used in this thesis for both trapezoidal and sinusoidal PM motors.

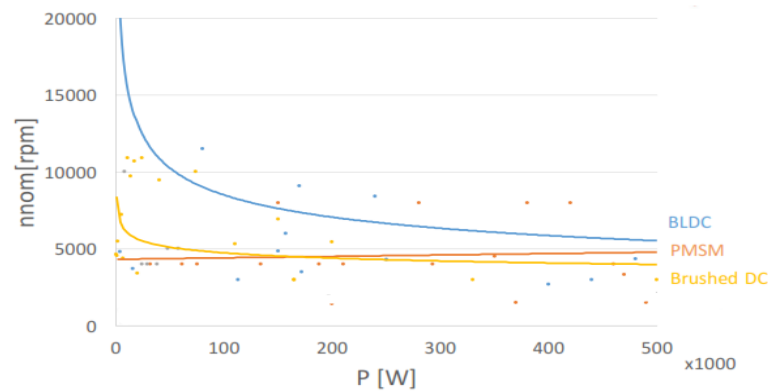


Figure 1.6 Motors operation with respect to Power vs. speed

Fuel Pump

As described in the first chapter, pump types and hydraulic flow rate and pressure calculation is needed for a sufficient fuel delivery to the engine. In this chapter fuel pump types according to their installation in automotive and structure is described. The regenerative turbine pump is selected for its advancement and then the mathematical modeling of regenerative turbine pump is described. Fuel type is explained at the end of the chapter because its characteristic data is needed for hydraulic calculation. Finally, at the end of the chapter hydraulic simulation with Simscape is done.

2.1 Automotive fuel pump types

Electrical fuel pump can be installed in-line or in-tank in an automotive fuel system to deliver fuel to engine. In-line fuel pump normally install under the vehicle that air flow cause temperature reduction of the fuel pump. In-tank fuel place inside the fuel that temperature of fuel pump doesn't increase due to the fuel existence in the tank, also it cause noise reduction, lubricating of the motor pump. In-line and in-tank fuel pump are shown in figure 2.1.

Vehicle with high-performance, like a model of Porsche have four fuel pump, and race engine that exceed 750 horsepower, also for truck that have two fuel tanks, two fuel pump are used one for each one. Dual channel pumps have two parallel rows of fuel pumps that feed high pressure fuel lines to the engine [26], but this fuel system isn't economical for normal automotive and it is used for some race car.

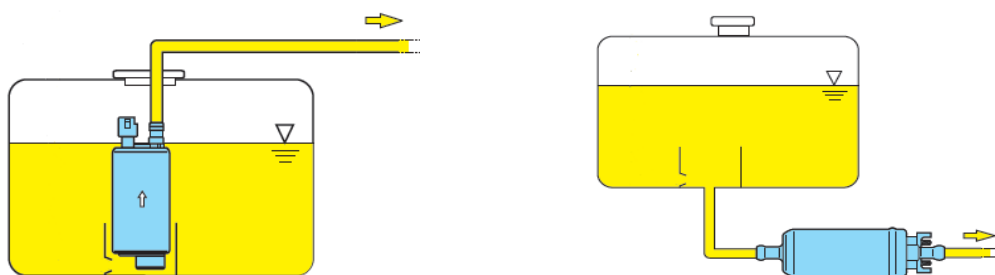


Figure 2.1 A) the left figure is an in-tank fuel pump B) the right pump is an in-line fuel pump

2.2 Pump types

In electronically fuel injected (EFI) engine, fuel pressure is changing due to engine work. Pressure is controlled by the ECM to increase the efficiency and performance of engine. When a great fuel pressure is needed for high performance applications, turbine and vane style pumps are often used, they use centrifugal force from a spinning rotor or turbine wheel inside housing thereby forcing fuel into the fuel line and engine.

Pump divides in many groups according to its flow's volume and the desired applications; here, the three types of pump are discussed, in order to know, that which one of them is a sufficient option for electrical fuel pump.

2.2.1 Positive displacement pump

With positive displacement pump fuel will be pumped by the constant rate. Its term of operation is that fluid flows into the suction with expanding cavity, then liquid exit from discharge port with decreasing cavity with respect to the suction port. The amount of fuel flow can be change by change of the rotation speed of the pump (motor). One of the most common type of positive displacement pump is rotatory vane pump that it is described in the following paragraph.

Rotatory vane pump

Rotatory vane pump is a type of positive displacement pump, and as it include in its name, it consists of vanes. It has circular rotor rotating inside a larger cavity. The centers of these two are offset from each other, causing eccentricity [30]. The fluid flow through the input port to the pump and then by rotation of rotor inside the cam ring, and then rotation vanes, the kinetic energy add to the fluid and then will discharge throughout the discharge pipe; the figure 2.2A, it is shown a vane pump. They are good pumps for high viscosity applications. Its advantages are running dry for short periods of time, sliding contact vanes make it good for low viscosity liquid and compensate for wear through vane extension. And its disadvantages are not suitable for viscosity fluid and pressure and complex design performance.

2.2.2 Variable displacement pump

In variable displacement pump the volume of flow rate per time can be change also in constant rotational speed of the pump. The most use of variable displacement pumps are in industry that the motors speed are constant. There are many types of variable displacement pumps, an example of them is axial piston pump.

2.2.3 Velocity pump or rotor-dynamic pump

Rotor-dynamic pumps deliver kinetic energy to fluid by increasing the flow velocity. The added energy to the fluid is converted to pressure, when the velocity is reduced prior to flow exit in the pump discharge port. The conversion of kinetic energy to pressure is described by Bernoulli's equation [29].

One advancement of rotor-dynamic pump as compare as to positive displacement pump is the pump operation when discharge valve or pipe is close and fluid delivery of the pump is zero. When the discharge valve close positive displacement pump will result in a continual build up in pressure resulting in mechanical failure of either pipeline or pump, but in rotor-dynamic pump can operate safely for a short time when the discharge is close [29].

One of the most use rotor-dynamic pump is centrifugal pump.

Centrifugal pump:

As it is explained before centrifugal pump is a rotor-dynamic pump. Centrifugal pump use impeller to add pressure and flow rate of the fluid. Normally fluid enter the casing of the pump from the center around of the rotating shaft, then flow radially or axially through the discharge port. Centrifugal pump is used for high delivery of fluid though smaller head and it is a good option for high speed fluid delivery. The centrifugal pump term of operation in shown in figure 3.2B.

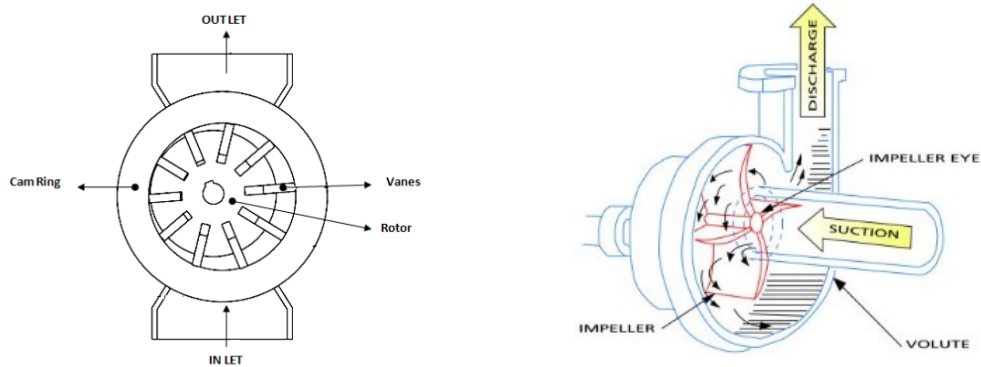


Figure 2.2 A) the left figure is a vane pump B) the right figure is a centrifugal pump

2.3 Regenerative turbine pump

Regenerative turbine pumps in some papers is part of positive displacement² pump, but in reality at low specific speed the pump have characteristics of positive displacement pump and centrifugal pump. The pressure increase as the exchange in momentum between the impeller and the fluid [28]. Regenerative turbine pump type is important especially in volatile fluids. If the volatile fluids allowed to flash to vapor during pumping, the collapse of entrained vapor bubbles create cavitation that cause severely damage of pump internal [27]. Regenerative turbine pump becoming popular pump for situations in which cavitation condition occur, such as during delivery of high-volatility fluid [27]. Regenerative turbine pump can offer a more efficient to other centrifugal pump in many applications. It is great pump to deliver high pressure with low flow rate fluid, and it has low cost and it is compact.

Regenerative turbine pump made of an impeller that vanes are installed at both end side of sealing, then they are covered by casting, that it is shown in figure 2.3. The vanes rotate with a shaft of the electrical motor. The casting is cover to the impeller and it consist path of fluid flow from suction to discharge, the flow path approximates toroidal helix, similar to the shape of corkscrew [28]. Suction and discharge of the pump is vertical with respect to the casting of the pump, this is a suitable design for flow entering and exiting from the pump, because the in-tank and also most inline pump cross fluid horizontally with respect to the pump installation.

² In some papers, regenerative turbine pump categorized as rotor-dynamic pump.

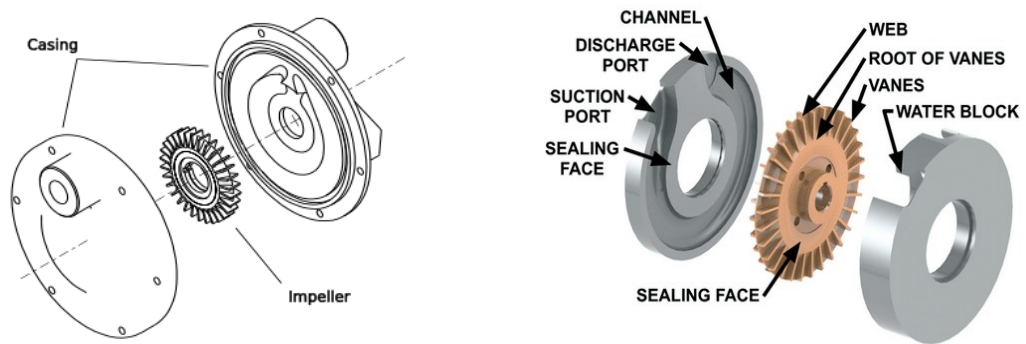


Figure 2.3 Regenerative turbine pump

Fluid travel in regenerative turbine pump takes many trips through the vanes when the fluid push through channel passageway. Circulatory flow is imposed on the fluid and it reaches the fluid channel periphery, it is then redirected by the specially shaped fluid channels, around the side of the impeller, and back into, where the process begin again. The multiple cycles through the turbine vanes are called regeneration, for this reason the pump is called regenerative turbine pump [31]. The rotation of fluid in passageway of casting between vanes is shown in figure 2.4.

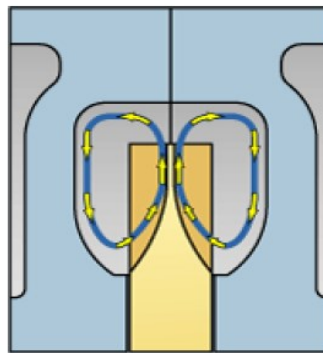


Figure 2.4 Fluid circulatory flow in regenerative turbine pump

The liquid is immediately picked up by the buckets and pumped about the ring channel. The fuel flow in complete model of fuel pump is shown in figure 2.5. As it is shown the fuel flow from the surrounding of electric motor that also cause the motor temperature reduction.

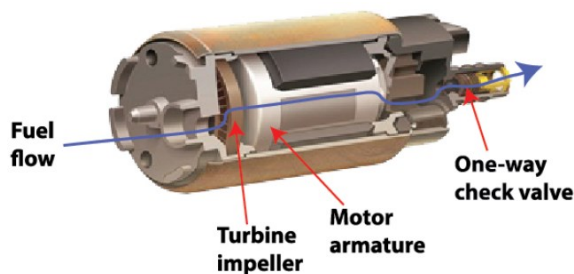


Figure 2.5 Overall view of fluid flow in a fuel pump

2.4 Mathematical Model of regenerative turbine pump

The pump pressure gain calculation is done by using reference [32]; where analytical approach is used. Also, with some assumption is that are: steady, incompressible flow and the number of circulation is equal to the number of the impeller blades excluding the part of stripper.

The head rise of the pump in per one circulation is calculated by equation 2.1.

$$gh_{cir} = \frac{A_{2t}V_{m2t}R_{2t}V_{u2t} + A_{2s}V_{m2s}R_{2s} - A_1V_{m1}V_{u1}R_1}{R_m A_c} \quad (2.1)$$

The total head of the pump H formula shown in equation 2.2, and the after that there is the head coefficient ψ equation 2.3.

$$H = nh_{/cir} - \frac{1}{2g} K_p \left(\frac{Q}{A_c}\right)^2 \quad (2.2)$$

$$\psi = \frac{gH}{N^2 D_{2t}^2} - K_p \varphi^2 \quad (2.3)$$

K_p is loss coefficient corresponding to the pressure drop.

φ is flow coefficient.

D_{2t} is hydraulic diameter.

$h_{/cir}$ head per circulation.

n is number of circulation (number of times the fluid passes through impeller blades).

The pump number of circulation n is calculated by the following formula. Where Z is the number of the blade and ϑ_{eff} is the effective angle of the pump.

$$n = \frac{\vartheta_{eff}}{360} Z \quad (2.4)$$

For calculation the hydraulic efficiency, the power input P_i and the real flow rate Q_r must be taken. The hydraulic efficiency is consider by

$$\eta_h = \frac{\rho Q_r g H}{P_i} \quad (2.5)$$

Losses calculation in the pump is important part of fluid power and flow rate calculation. Losses are categorized as follow [32], but here the incident losses that caused by the difference between the blade angle and the flow and is not calculated.

- Tangential head loss in the side channel h_c is calculated in the equation 2.6, as V_c is the average tangential velocity in the side channel and ξ_c is the channel skin friction loss that it earn by the equation 2.7. Where D_h the hydraulic diameter of side channel and L is the diameter of side channel.

$$gh_c = \frac{1}{2} \xi_c V_c^2 \quad (2.6)$$

$$\xi_c = \lambda_f \frac{D_h}{L} \quad (2.7)$$

$$\lambda_f = \lambda_o [1 + 0.075 Re^{0.25} \left(\frac{D_h}{2R_t} \right)^{0.5}] \quad (2.8)$$

$$\lambda_o = 0.316 Re^{-0.25} \quad (2.9)$$

- Direct loss in the impeller h_i and it consist losses due to turning, contraction, friction and sudden expansion. It is proportional to the relative velocity in the impeller. In the following equation 2.10, ξ_i is loss coefficient that it is taken experimentally.

$$gh_i = \frac{1}{2} \xi_i W_{2t}^2 \quad (2.10)$$

The summation of the two above losses, it earned the total friction power losses P_f , that it is,

$$P_f = \rho g Q_c (h_i + h_c) \quad (2.11)$$

The fluid power

The fluid power result of the pump is the power added by the impeller and then subtraction of losses in the input and output port [32].

$$H = H_c - H_{ic} \quad (2.12)$$

H_c is total head imparted from the impeller.

H_{ic} is head loss in the inlet and outlet ports.

Total power deliver from the impeller P_c is shown in the following equation.

$$P_c = \rho g Q H_c \quad (2.13)$$

Finally, the total power is calculated by

$$P_i = P_c + P_f \quad (2.14)$$

Leakage flow rate

The leakage flow cause reduction flow in the pump. The leakage flow can be calculated by the following formula [32].

$$Q_l = C_d A_{cl} \sqrt{2gH} \quad (2.15)$$

Then the friction drag coefficient C_d is calculated.

$$C_d = \frac{1}{\sqrt{\lambda_f (L/D_h) + 1.5}} \quad (2.16)$$

A_{cl} is clearance area.

And finally the total flow rate Q_r delivered by the pump is

$$Q_r = Q - Q_l \quad (2.17)$$

2.5 Fuel

Fuels are used for vehicle also they are called motor fuel. Motor fuel provide power to motor vehicle. Majority of motor vehicle are powered by gasoline (petrol) or diesel. Other energy sources for fuel delivery to motor and they become popular are biodiesel, compressed natural gas (CNG) and etc. Here gasoline, diesel the two most useful fuels are described [33] that also need pump for delivery fuel to the engine.

- **Gasoline:**

Gasoline is used primarily as a fuel in spark-ignited internal combustion engines. Gasoline types use in EU (Europe) are Eurosuper-95, Eurosuper-98 (both lead-free) and in USA they are Regular (97 RON) and premium (95 RON). Its density is 750 kg/m^3 (from 720 kg/m^3 to 760 kg/m^3 at 20°C), and its thermal expansion is $900 \cdot 10^{-6} \text{K}^{-1}$. Its vapor pressure is typically 70 KPa at 20°C (from 50 to 90 KPa). Theoretical air/fuel ratio is $14.5 \text{ kg air by fuel}$. Finally its viscosity of gasoline is $0.5 \cdot 10^{-6} \text{ m}^2/\text{s}$ at 20°C [34].

- **Diesel:**

Diesel is used in diesel engine, whose ignition take place, without any spark, as result of compression of inlet air mixture and then injection of fuel [33]. The typical diesel types that are used in EU is type A that use for vehicles, and in USA is Distillate (Kerosene). The characteristic of such kind of diesel is described here. Typical density is 830 kg/m^3 (normally from 780 kg/m^3 to 860 kg/m^3 at 40°C). Its viscosity is $3 \cdot 10^{-6} \text{ m}^2/\text{s}$ (normally between $2 \cdot 10^{-6}$ to $4 \cdot 10^{-6} \text{ m}^2/\text{s}$). And the vapor pressure is 1 to 10 KPa at 38°C for diesel fuel.

The fuel that is selected from Simscpae library for simulation hydraulic in the pump is gasoline, and its specifications at 25°C are as following.

Viscosity: 0.563139 kg/m^3

Density: 715.312 cSt

Bulk modulus at atm. Pressure and no gas: $1.13289e + 09 \text{ Pa}$

Relative amount of trapped air is assumed: 0.005

2.6 Mathematical modeling in Simscape

As described in the first section the fixed displacement pump is selected for this topic. Now, the working principle of the pump is described below [1].

The generated volumetric flow rated by the pump is calculated:

$$q = q_{ideal} - q_{leak} \quad (2.18)$$

q is volumetric flow.

Q_{ideal} is ideal volume flow rate

Q_{leak} is leakage flow rate of the pump

$$q_{ideal} = D \cdot \omega \quad (2.19)$$

$$q_{leak} = K_{leak} \cdot p \quad (2.20)$$

K_{leak} is the leakage fiction coefficient

$$K_{leak} = \frac{K_{hp}}{v \cdot \rho} \quad (2.21)$$

K_{HP} is the Hagen-Poiseuille coefficient for laminar pipe flows. This coefficient is computed from the specified nominal parameters.

$$K_{hp} = \frac{D \cdot \omega_{nom} \cdot (1 - \eta_w) \cdot v_{nom} \rho_{nom}}{p_{nom}} \quad (2.22)$$

And for torque calculation of the pump:

$$\tau = \tau_{ideal} + \tau_{fiction} \quad (2.23)$$

$$\tau_{ideal} = D \cdot \Delta p \quad (2.24)$$

D is the specified value of the Displacement block parameter.

ω is the instantaneous angular velocity of the rotary shaft.

Δp is the instantaneous pressure gain from inlet to outlet.

The Simulink model of the pump is shown in figure, where the input S is the rotational input of the pump. The pressure gain is calculated by the analytical method and then the fixed displacement pump is used for simulation with data of generative turbine pump.

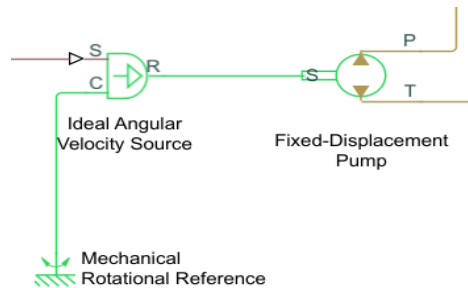


Figure 2.6 Pump and velocity source of the pump in Simscape

In order to know the simulation result and also for feedback control of the pump, the fluid measurement of the system is needed, pressure and flow rate sensor is used the pressure in order to achieve this goal. In figure, 2.7, the overall Simscape model of hydraulic is shown.

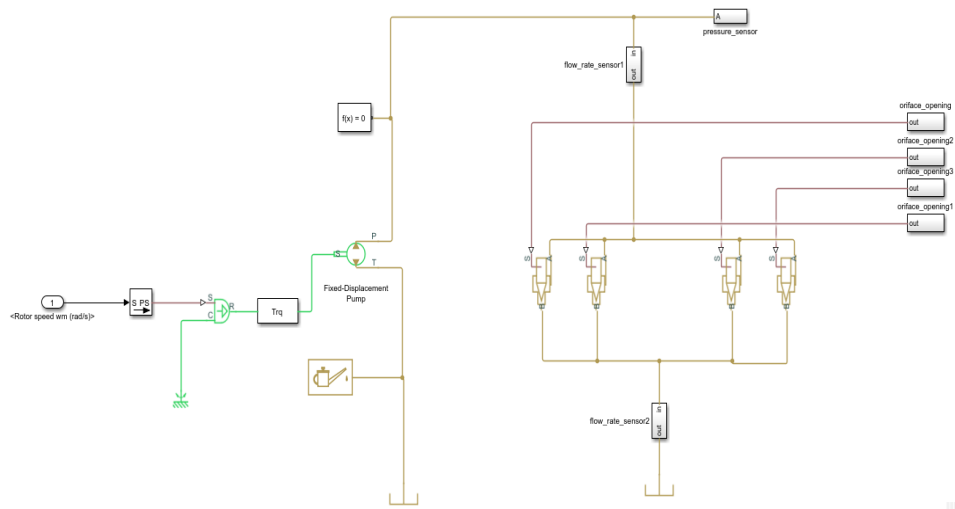


Figure 2.7 Hydraulic Simscape model

Brushless Motor and Mathematical Modeling

This chapter describe working principle of brushless motor. Brushless motor for its operation need an inverter. Normally, for three-phase brushless motor two-level inverter is used. SVM is describe as a gate signal input to the inverter. A brief review of control of the brushless motor is discussed and also different types of control. Mathematical modeling of brushless motor is also described. At last, the brushless motor parameters that it is used for this thesis is shown and also some of parameters that they do not presented in the datasheet is calculated.

3.1 Brushless (BLDC) motor operation

BLDC motor for its operation need power device for electricity supply, sensor for rotor position detection and other measurement device in case of sensorless operation and controller. Unlike brushed dc motor, the BLDC motor doesn't work with direct electricity supply to the motor, it need inverter to supply three-phase voltage. Inverter is also control the BLDC motor with switching of transistor, but the control signal for controlling the inverter is coming control unit. The control algorithm is implemented to the control unit. The desired parameters that are needed for control section are supplied to the control unit by sensor or other measurement device. In figure 3.1, the devices that are needed for motor operation is shown. And they are described in detail in following sections.

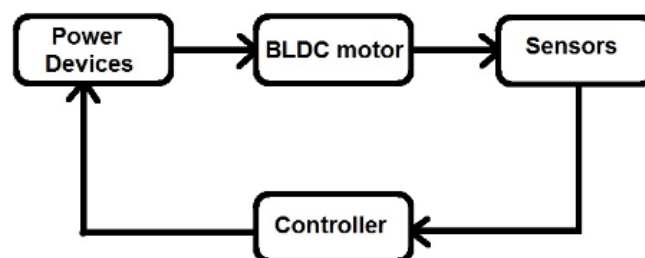


Figure 3.1 BLDC motor term of operation

3.1.1 Inverter

For three phase BLDC motor six-step inverter is used, it is shown in figure 3.2. The inverter is three phase semiconductor bridge. Commutation in BLDC motor is created by the electronic inverter. In every constant time two phase out of three phase that supply the stator is active, while one phase is off.

The two phases are on as feedback signal of the hall sensor. When each time a magnet pass true the sensor; the sensor send a signal to the controller, and controller can implement the correct sequence for motor control. In figure3.2, six sequence of six-step inverter in shown. The downside of trapezoidal (six-step) commutation is that it results in torque ripple at each step of the commutation every 60 degree in trapezoidal PM motor.

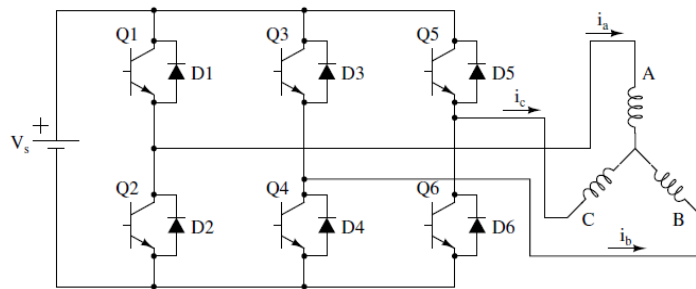


Figure 3.2 Six-step inverter

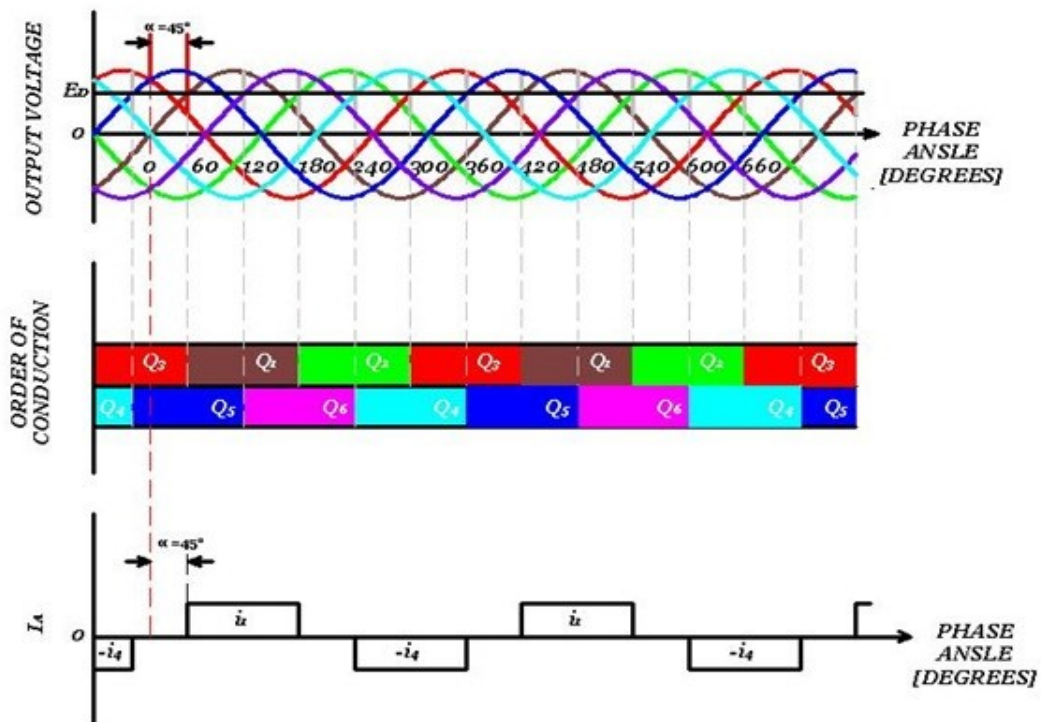


Figure 3.3 Inverter operation result

3.1.1.1 Snubber circuit

Snubber is energy-absorbing circuits that is used to suppress the voltage spike caused by the circuit's inductance during switching. The most common snubber circuit is a capacitor and resistor connected in series that it is named RC snubber.

In the figure, and IGBT/diode circuit in parallel is shown that it is used for inverter. In figure 3.4 and figure 3.5, the result of IGBT/diode operation is shown. As it is clear in the figures, there is voltage and current overshoot in operation.

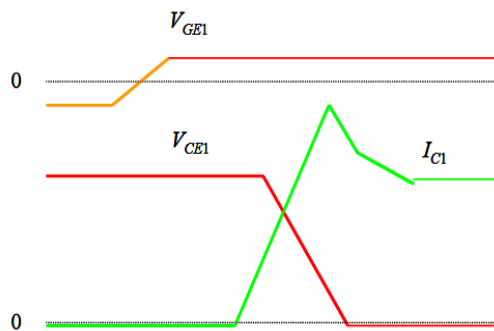


Figure 3.4 Switch on

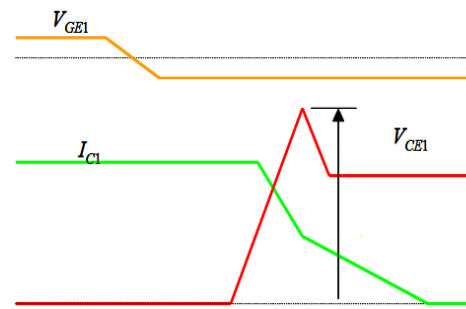


Figure 3.5 Switch off

In figure 3.6, RC snubber circuit is shown that is used with transistor. In three-phase inverter because of usage transistor the RC snubber circuit is needed to avoid fault in transistors and diode due to the voltage and current rising. Because of this reason on the Simulink model of the two-level inverter, the snubber circuit resistor and capacitor values are needed.

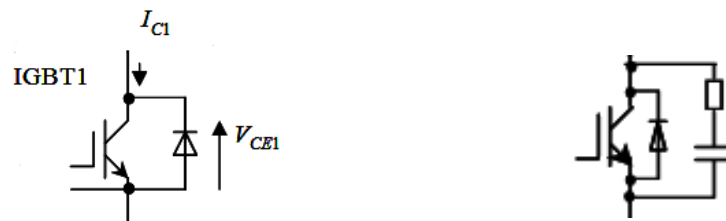


Figure 3.6 IGBT/Diode switching without snubber and with snubber

3.1.2 Control

BLDC motor is not a direct drive motor that operate directly with voltage supply. A control part is needed for operation of BLDC motor. The output power for such type of motors is not smooth; however, ripples appear due to the inherent inductance of the winding which prevents current from rising or diminishing instantaneously [7].

BLDC motor are mostly used in applications that need wide speed range. And there is different control algorithm for controlling BLDC. FOC is best control method for wide speed range. But FOC steady state stability and torque ripple as compare to DTC are its disadvantage. Also in the past the computation of FOC was a problem due to the high computation requirement; now by

the new technology of chipset this problem is overcome. This is a method in which the current vector (magnitude and direction) is determined relative to the rotor, rather than on the basis of sinewaves, as is done in sinusoidal commutation. While sinusoidal commutation has low efficiency at high speeds, FOC provides high efficiency across a wide speed range, as well as very smooth motion.

3.2 Fundamental of BLDC motor

BLDC motor rotor is made of permanent magnet and stator consist of coils, it is shown in figure 3.7. The main advantage of BLDC motor is usage of electrical commutator instead of mechanical commutator that is used in brushed DC motors. Electrical commutator used to commutate specific current to coils, it is more efficient, long life and faster with respect to mechanical commutation. Compared with other kinds of motors, the trapezoidal PM motor is excited by a square wave, so that the motor has lots of advantages, such as higher permanent magnet utilization, smaller size, larger motor torque, higher efficiency and reliability [10]. Sinusoidal PM motor is excited with sinusoidal waves. BLDC motor generally made of three parts: motor structure, sensor detection, electronic commutation.

Current passing through stator and create magnetic fields, then stator magnetic field interact with rotor magnetic fields. The magnetic fields of stator cause interaction of rotor magnetic fields, for these purpose the current by inverter (electronic commutator) must apply properly to the stator coils. The direction of main stator magnetic field is perpendicular to rotor magnetic field [10]. These force attraction create torque that cause movement (rotation) of the rotor. A control circuit is needed to control the current and voltage supply to motor (stator), for this achievement control circuit need rotor position. Rotor position is provided by Hall Effects sensor. Also it is possible to use sensorless BLDC motor, it is considered in section 3.2.3.

3.2.1 Stator

Stator consist of symmetric windings (coils) that are one-phase or multi-phase. Stator is connected in Y or Δ type. The major difference between the two patterns is that the Y pattern gives high torque at low RPM and the Δ pattern gives low torque at low RPM. This is because in the Δ configuration, half of the voltage is applied across the winding that is not driven, thus increasing losses and, in turn, efficiency and torque. The most useful connection because its performance and cost is in Y connection type which is more three-phase [10, 11].

Steel laminations is two type: slotted and slot less. The slot less has lower inductance and it can run at very high speed. In slot type when the teeth of stator align with rotor permanent magnet causing creation of cogging torque that create ripple in speed.

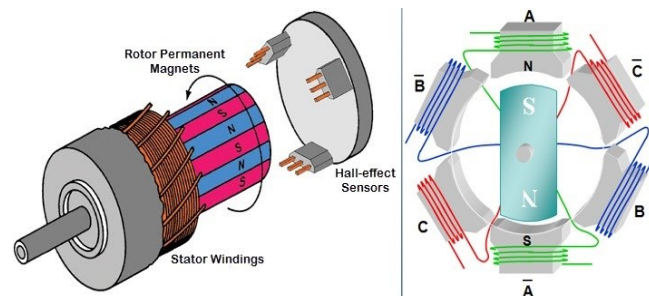


Figure 3.7 BLDC motor

3.2.2 Rotor

Rotor consist of permanent magnet and with certain poles. Number of poles increase torque of motor but at cost of reducing maximum speed of motor [11]. The BLDC motor rotor are usually surface mounted and magnet embedded rotor. In surface mounted rotor the magnets are place as tile-shaped in surface of rotor mostly in rectangle strip to reduce the cost. The designer always adopts this structure with its pole arc width larger than 120 degree electric angle in order to generate a square air gap flux density and decrease torque ripple [10].

Magnet-embedded rotor. When the rectangular permanent magnets are embedded into the iron core of the rotor, we call it a magnet-embedded rotor. Since the magnetism gathering technology can provide larger flux, the flux under one polar pitch is produced by two adjacent poles in parallel. In this case, magnetism-isolating technology or a stainless steel shaft should be adopted [10].

3.2.3 Sensor

Hall Effect sensors provide electrical signal to provide rotor position to control part, it is shown in figure 3.8. The magnetic field insert force into the electric current and push the current flowing in a side of the conductor and cause potential different in the sensor. There are many kind of Hall Effect sensor. Magnetic type sensor has the advantages of compact volume, low price and convenient operation. Therefore, it is commonly used in BLDC motor control systems as the rotor-position detector [10]. Normally the sensor produce three digit number as feedback that change every 60 degree.

The disadvantage of the BLDC with sensor is high cost due to the sensor and wiring cost, increasing motor volume, also Hall Effect sensors are temperature sensitive and because of that operation of motor is limited; these cause decreasing in system reliability because of extra component and wiring.

Moreover, automobiles usually have strict restrictions for the volume of the motor. However, sensors are usually installed inside the motors, which will increase the volume. Consequently, the sensor less control strategy will be an important development direction of automotive BLDC motor drive systems. There are different ways for estimation of rotor position.

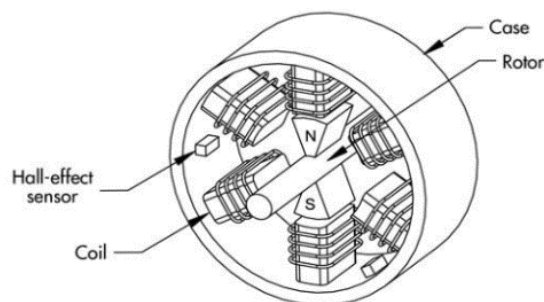


Figure 3.7 Hall Effect sensor in BLDC motor

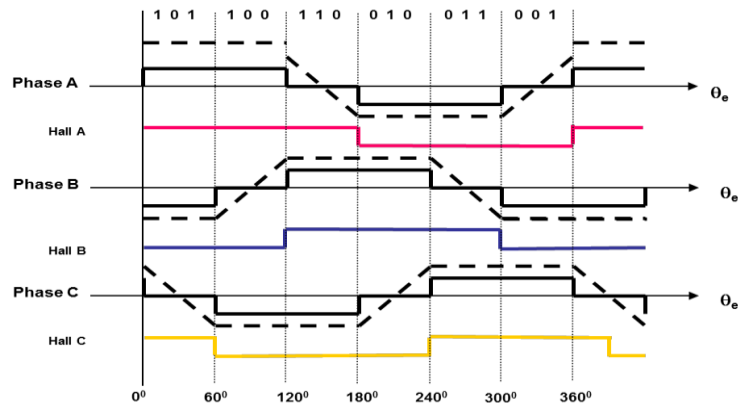


Figure 3.8 Sensor signal of trapezoidal PM motor

3.2.4 BEMF (back electromotive force)

By current passing through stator coils flux linkage is created, flux linkage changing by rotation of magnet. Back-emf is very dependent on the waveform of flux linkage [12, 7]. Trapezoidal PM motor have trapezoidal Back electromotive force (BEMF); it is the difference with sinusoidal PM that have sinusoidal back-emf. And although in theory, the trapezoidal PM motor's back-emf is trapezoidal, in reality, the back EMF waveform is not purely trapezoidal because of inductance in the motor smooths the back EMF [7]. In sinusoidal BLDC motor (surface mounted PMSM) back-emf is sinusoidal. Both trapezoidal and sinusoidal back-emf is shown in figure.

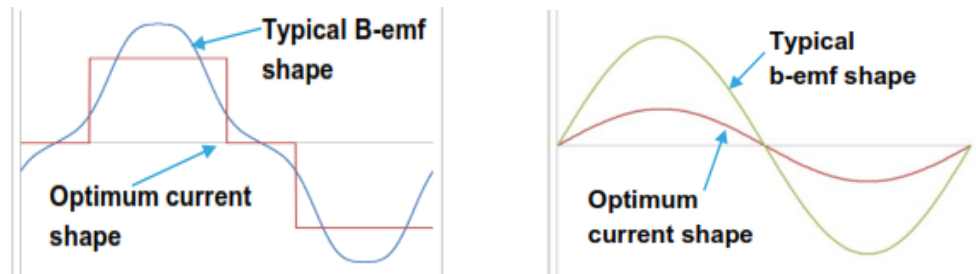


Figure 3.9 A) Left figure is trapezoidal back-emf B) Right figure show Sinusoidal back-emf

3.3 Mathematical model

As described in the previous section, the most popular BLDC motor is three phase motors, also most of them are with Y connected wiring, 120 degree electrical. Winding are placed in ferromagnetic material in stator. Rotating magnet induce voltage in winding, this create and inductance (L) that oppose the rate of change of current [10, 12]. Resistance in wiring also cause voltage drop in stator. Simplified model circuit of BLDC is shown in figure 3.10. The V_a , V_b , V_c represent three phase of BLDC motor. This dynamic model is described with assumption that induced current due to the harmonic field are neglected and iron and stray losses are also neglected.

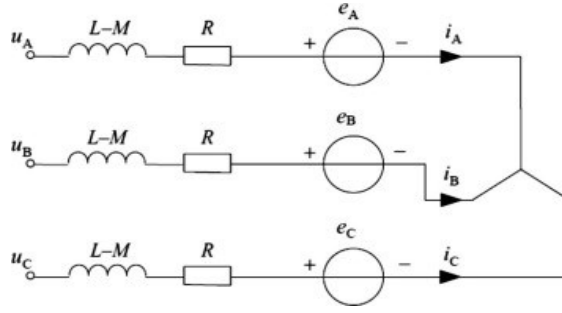


Figure 3.10 Simplified model of brushless PM motor

The following equation can be derived from the equivalent circuit:

$$T_e = b\dot{\theta} + J\ddot{\theta} + T_l \quad (3.1)$$

$$V_{ab} = R(i_a - i_b) + L \frac{d}{dt}(i_a - i_b) + e_a - e_b \quad (3.2a)$$

$$V_{bc} = R(i_b - i_c) + L \frac{d}{dt}(i_b - i_c) + e_b - e_c \quad (3.2b)$$

$$V_{ca} = R(i_c - i_a) + L \frac{d}{dt}(i_c - i_a) + e_c - e_a \quad (3.2c)$$

Here T_e , $\dot{\theta}$, b , J , T_l , V , R , L and e denote the electrical torque, the mechanical rotational speed, the viscous friction constant, the rotor inertia, the mechanical load torque, the phase-to-phase voltage, the phase resistance, the phase inductance and the phase BEMF respectively. Notice that the voltage and current have following relationships:

$$V_{ab} + V_{bc} + V_{ca} = 0 \quad (3.3)$$

$$i_a + i_b + i_c = 0 \quad (3.4)$$

If there is change in the rotor reluctance with angle, and assuming symmetric three phases, the self-inductances of all phases are equal and the mutual inductance between phases are equal to one another and they are denoted [12] as

$$L_{aa} = L_{bb} = L_{cc} = L \quad (3.5)$$

And

$$L_{ab} = L_{ba} = L_{ac} = L_{ca} = L_{bc} = L_{cb} = M \quad (3.6)$$

For simplification the two voltage equations are needed:

$$2V_{ab} + V_{bc} = 3Ri_a + 3L \frac{d}{dt}i_a + 2e_a - e_b - e_c \quad (3.7a)$$

$$-V_{ab} + V_{bc} = 3Ri_b + 3L \frac{d}{dt}i_b + 2e_b - e_a - e_c \quad (3.7b)$$

The torque equation for three phase can be written:

$$T_e = (e_a i_a + e_b i_b + e_c i_c) / \dot{\theta}_m \quad (3.8)$$

The trapezoid back-emf can be expressed:

$$e_a = \frac{k_e}{2} \dot{\theta}_m \text{Tra}(\theta_e) \quad (3.9a)$$

$$e_b = \frac{k_e}{2} \dot{\theta}_m \text{Tra}(\theta_e - \frac{2}{3}\pi) \quad (3.9b)$$

$$e_c = \frac{k_e}{2} \dot{\theta}_m \text{Tra}(\theta_e - \frac{4}{3}\pi) \quad (3.9c)$$

Here, k_e is the BEMF constant and θ_e is the electrical angle which is equal to the mechanical angle times the number of pole pairs ($\theta_e = p\theta_m$). (θ) is the trapezoidal waveform function and one period of the function can be described as follow:

$$F(\theta_e) = \begin{cases} 1, & 0 \leq \theta_e < \frac{2\pi}{3} \\ 1 - \frac{6}{\pi}(\theta_e - \frac{2\pi}{3}), & \frac{2\pi}{3} \leq \theta_e < \pi \\ -1, & \pi \leq \theta_e < \frac{5\pi}{3} \\ 1 + \frac{6}{\pi}(\theta_e - \frac{2\pi}{3}), & \frac{5\pi}{3} \leq \theta_e < 2\pi \end{cases} \quad (3.10)$$

Further, we can simplify Equation 5 using Equation 6, 7, 8, and we can derive the following equation which makes the modelling more convenient:

$$T_e = \frac{K_e}{2} (\text{Tra}(\theta_e) x i_a + \text{Tra}(\theta_e - \frac{2}{3}\pi) i_b + \text{Tra}(\theta_e - \frac{4}{3}\pi) i_c) \quad (3.11)$$

The equation of motion for a simple system with inertia J, friction coefficient B [12], is

$$J \frac{d\omega_m}{dt} + B\omega_m = (T_e - T_1) \quad (3.12)$$

And electrical rotor speed and position relation are

$$\frac{d\theta_r}{dt} = \frac{P}{2} \omega_m \quad (3.13)$$

P is the number of poles

ω_m is the rotor speed in mechanical rad/s

θ_r is the rotor position in rad

For sinusoidal BLDC motor where the trapezoidal is used the equation is different, also in some reaserch paper these equation is used for trapezoidal BLDC motor that also in this thesis is used. In datasheet of the trapezoidal and sinusoidal BLDC motors that quadrature inductatnce (L_d) and direct inductance (L_q) have equal values, but in reality they have diferrent values that if field oriented control is not used the difference in reslut is not to much. In this thesis because the effcinet result is needed these the difference of these values calculated during calculation. The equations of direct and quadrature current and torque are

$$\frac{d}{dt} i_d = \frac{1}{L_d} v_d - \frac{R}{L_d} i_d + \frac{L_q}{L_d} p\omega_m i_q \quad (3.14a)$$

$$\frac{d}{dt} i_q = \frac{1}{L_q} v_q - \frac{R}{L_q} i_q + \frac{L_d}{L_q} p\omega_m i_q - \frac{\lambda p\omega_m}{L_q} \quad (3.14b)$$

$$T_e = 1.5p[\lambda i_q + (L_d - L_q)i_d i_q] \quad (3.14c)$$

Where, λ is amplitude of the flux induced by the PM of the rotor in the stator phases.

3.4 Motor Parameters:

The BLDC motor parameters that is used for simulation is shown in table 3.1. Also the motor datasheet is available in appendix 2.

Parameter	Motor data
Maximum power	60 W
Nominal voltage	12 V
Nominal current (max. continuous current)	4.72 A
Terminal resistance phase to phase	0.447 Ω
Terminal inductance phase to phase	0.049 mH
Torque constant	14.2 mNm/A
Speed constant	440 rpm/V
Nominal torque (max. continuous torque)	63.6 mNm
Stall torque	381 mNm
Stall current	26.8 A
Rotor inertia ³	21.9 gcm ²
Poles pairs	1

Table 3.1 Motor parameters

According to manufacture information the L_q is equal to half of the phase to phase inductance of the motor.

$$L_q = \frac{1}{2}(L_{ph-ph}) \quad (3.15)$$

Thus the value of L_q is equal to 0.2.45e-05 H.

And for EC-I motor model of Maxon motor company, L_d (quadratic inductance) value is bigger than L_q ($L_d > L_q$), and it is ten percent more than L_q . In this EC model motor is used, and it is assumed ten percent difference of L_q and L_d . Thus the value of L_d is equal 2.205e-05 H.

The phase to phase resistance is provided by the motor datasheet. The motor is wye connected winding and the stator resistance can be calculated according to the following formula.

$$R_s = \frac{R_{s,s}}{2} = 0.2235 \Omega \quad (3.16)$$

Parameters like voltage constant (K_e) and magnetic flux (Ψ) that they are not represented in the datasheet is earn from the Simulink parameters calculation of motor, and they are

$$K_e = 0.00171706 \text{ V}_{\text{eak } L-L} / \text{rpm}$$

$$\Psi = 0.0094667 \text{ V.s}$$

³ gcm² is gram centimeter square, it is moment of inertia unit.

Analysis of brushless motor for simplicity and accuracy is based on these assumptions: stator resistances of all the winding are equal, self and mutual inductances are constant, semiconductor devices in the inverter are ideal, iron losses are negligible, and temperature change affect is not taking into consideration.

Field Oriented Control

In chapter three FOC was selected as suitable control of brushless motor. In this chapter FOC is described in detail. Current control, speed control is designed and the stability of these control are described. MTPA is used for quadrature current creation and for achieving maximum torque that can produce with available current. And at the end of the chapter field oriented control is calculated and simulated with Simulink for achieving maximum reference speed which is above speed limit.

4.1 Vector reference frame

Mainly three reference frame is used in control of BLDC motor. One is in rotor and two other are located in stator. $\alpha\beta$ reference frame consist of three vector that they have 120 degree angle between adjacent vectors. Each of three vector are aligned with each stator winding pair. It make easy to understand current and voltage magnitude for each phase of stator. In three phase motor the only input to the motor is three phase voltage and current. In sensorless BLDC motor the measurement of these three phase are used.

There another vector d and q that are rotor reference frame. And there is 90 degree between components and the angle between d and q depends to the number of poles BLDC motor. This means that if BLDC motor made of two poles $\alpha\beta$ and dq have the same physical angle between its components, the difference is that dq frame is rotating by rotor. The vector frames are shown in figure 4.1. Also there possibility to change the frame from one to another that in the following section is described.

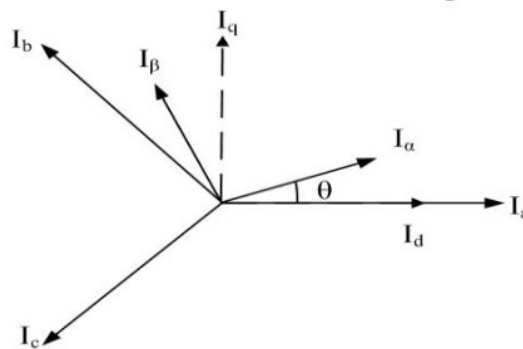


Figure 4.1 Vector reference frame

4.1.1 Clark Transformation

In two dimension working with vector is better to calculate and understand. In vector calculation there is possibility to convert the three vector frame to two vector frame without taking relation to phases and stator coils. The two phase out of three phase is measured and the third phase (i_c) is calculated by instantaneous relation:

$$i_a + i_b + i_c = 0 \quad (4.1)$$

The two currents i_α and i_β represents the two "new" currents for torque and flux respectively. For these purpose the Clark transformation is used to transform a/b/c to two vector frame that name $\alpha\beta$ frame. The α Vector is aligned to a vector from a/b/c frame and the β vector is orthogonal to the α vector reference frame.

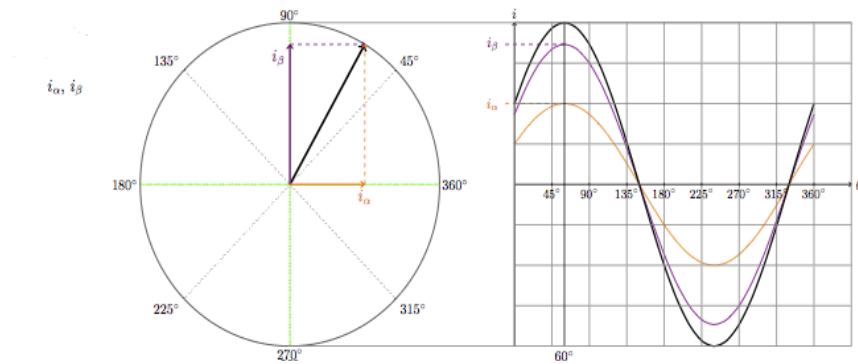


Figure 4.2 Clark transformation

The following equation is used for this transformation (s can be voltage vector or current vector).

$$i_\alpha = i_a \quad (4.2)$$

$$i_\beta = \frac{1}{\sqrt{3}} i_a + \frac{2}{\sqrt{3}} i_b \quad (4.3)$$

And Simulink model is

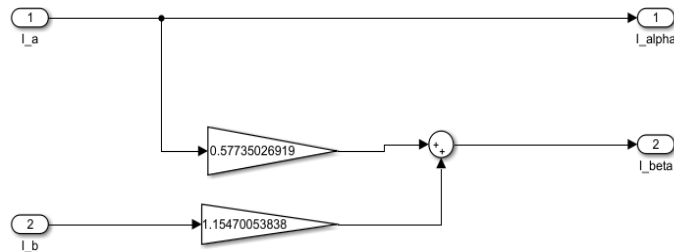


Figure 4.3 Simulink model of Clark transformation

4.1.2 Inverse Clark transformation

Also there is the possibility to transform the $\alpha\beta$ to A/b/c frame that it is called inverse Clark transform. The following equations are used for these transformation (s can be voltage vector or current vector).

$$V_a = V_\alpha \quad (4.4)$$

$$V_b = -\frac{1}{2}V_\alpha + \frac{\sqrt{3}}{2}V_\beta \quad (4.5)$$

$$V_c = -\frac{1}{2}V_\alpha - \frac{\sqrt{3}}{2}V_\beta \quad (4.5)$$

4.1.3 Park Transformation

The transformation time variant of $\alpha\beta$ vector frame to dq vector are done by Park transformation. The equations for this transformation are

$$i_d = i_\alpha \cos \theta + i_\beta \sin \theta \quad (4.6)$$

$$i_q = -i_\alpha \sin \theta + i_\beta \cos \theta \quad (4.7)$$

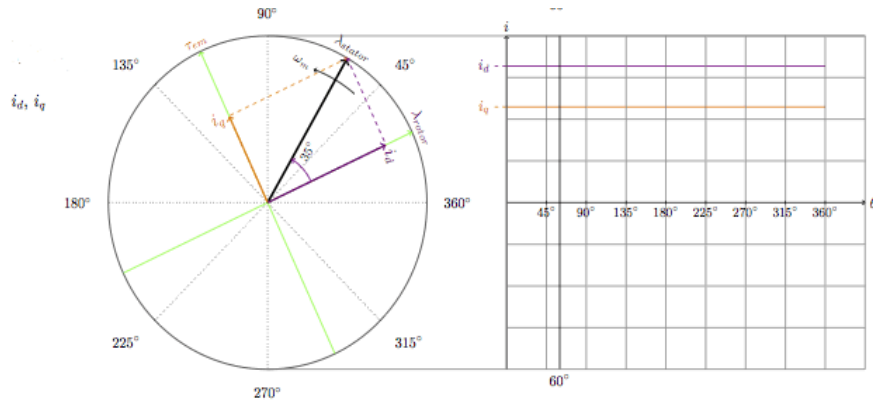


Figure 4.4 Park transformation

4.1.4 Inverse Park Transformation:

The dq vector transformation to $\alpha\beta$ is done by inverse Clark transformation, that formula is used for calculation of this transformation.

$$V_\alpha = V_d \cos \theta - V_q \sin \theta \quad (4.8)$$

$$V_\beta = V_d \sin \theta + V_q \cos \theta \quad (4.9)$$

Then, its Simulink model is shown in the following figure

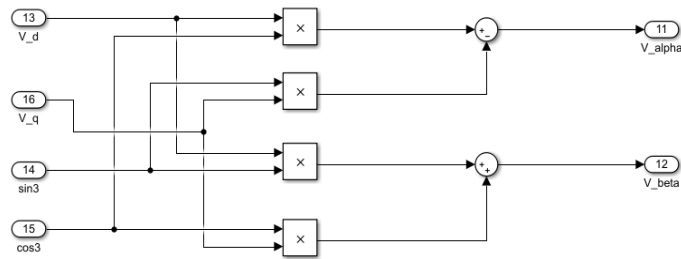


Figure 4.5 Simulink model of Park transformation

And the overall view of FOC is shown in figure 4.6, after park transformation the control is done and after that the controlled signal transformed by inverse Park and inverse Clarke transformation into the desired current or voltage.

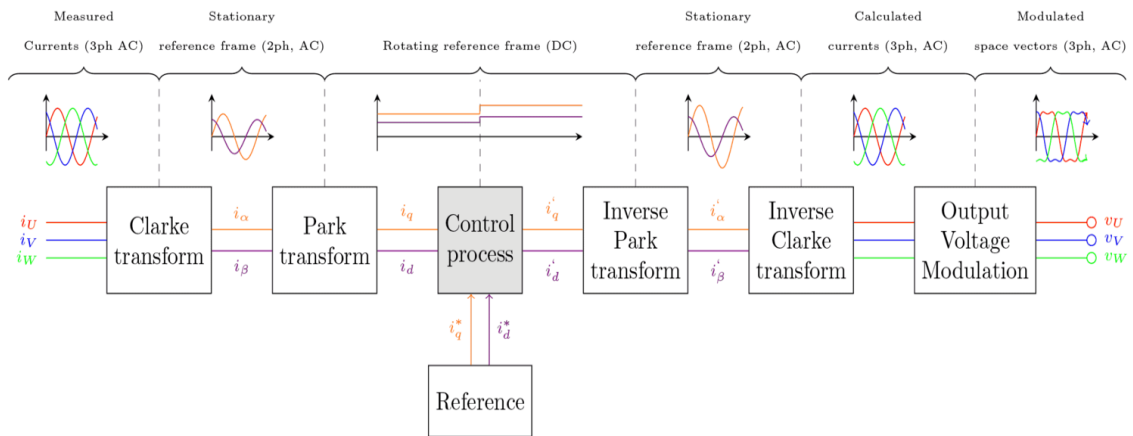


Figure 4.6 Overall view of vector transformation

4.2 Space vector modulation

Space Vector Pulse Width Modulation (SV-PWM) is a *modulation scheme* used to apply a given *voltage vector* to a three-phased electric motor. The goal is to use a steady state DC-voltage and by the means of six switches inverter emulate a three-phased sinusoidal waveform where the frequency and amplitude is adjustable [14].

As it is described in inverter section, in every time one of switches (transistors) from every leg is turn on. There is three leg in and the possible switches are $2^3 = 8$. Six of these vectors are called basic vector and represent voltages and two other are called zero vector that are located in zero voltage. The origin of the angles are the windings physical location inside the stator; installed around the circumference at 120° apart [14]. These vector can be represent as eight binary number that are represented in figure 4.7.

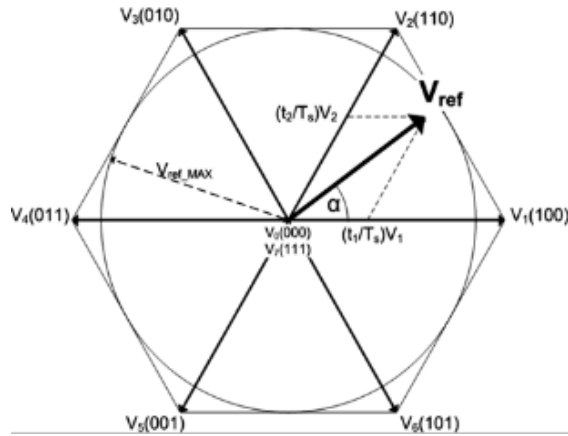


Figure 4.7 Space vector modulation performance

The two zero vectors V_0 and V_7 are also used to add dead time to the switching pattern. This dead time reduces the voltage magnitude and is necessary when the voltage reference magnitude is less than 100%. Between each transition only one switch is being changed. This greatly reduces harmonics in the motor which cause overheating and torque fluctuations [14].

The SVPWM (space vector pulse with modulation) is recently most used in inverter control because of easy digital realization, higher output voltage than regular SPWM under the same dc link voltage and less harmonics in the output voltage, [15].

An algorithm used for SVPWM used in [15, 16] is used for implementation SVPWM that it is shown in the figure 4.8. It is consist of four parts that are sector identification, vector action time, computation of switching time and PWM generation. The algorithm is simple due to elimination of complex trigonometric calculations and use of simple logic operation.

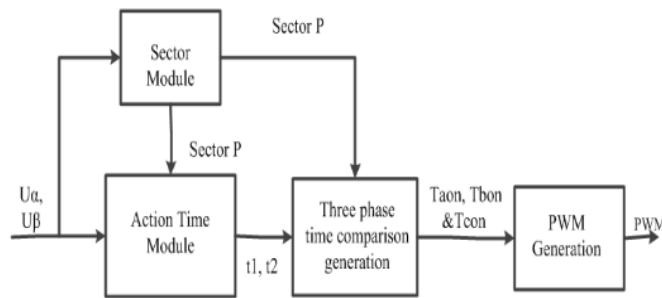


Figure 4.8 Space vector pulse with modulation

4.3 Current Control

The torque of the motor is depend to the current, thus the torque is controlled with current control. The torque is directly depend to the quadrature current (i_{sq}), and the direct current is used for flux control that it is described in the field weakening section.

The error between the measured dq and reference dq is the input of PI controller. The output of the PI controller is the corresponding d and q voltages. For individually control each current loop of i_{sd} and i_{sq} the decoupling term is used. The decoupling term Ψ , the Back-EMF, is depicted for 2 voltage equation of the BLDC motor [18]. Decoupling is important especially in high speed

range of motor. Also it eliminate cross coupling term that caused by mutual inductance in two control loop, and also decrease the peak current [22]. Also the current control with decoupling term shown in figure 4.8, and the equations are:

$$U_{sd} = R_s i_{sd} + \frac{d\Psi_d}{dt} - \omega_e \Psi_q \quad (4.10)$$

$$U_{sq} = R_s i_{sq} + \frac{d\Psi_q}{dt} - \omega_e \Psi_d \quad (4.11)$$

The two equations are coupled by the back-EMF, by subtracting this term the two current loops, the can be controlled independently. The voltage equations in s plane are:

$$U_{sd}(s) = R_s i_{sd}(s) + s L_d i_{sd}(s) \quad (4.12)$$

$$U_{sq}(s) = R_s i_{sq}(s) + s L_q i_{sq}(s) \quad (4.13)$$

The transfer function of BLDC motor for d and q current loop are:

$$P_d(s) = \frac{1}{s L_d + R_s} = \frac{1}{R_s (s T_{sd} + 1)} \quad (4.14)$$

$$P_q(s) = \frac{1}{s L_q + R_s} = \frac{1}{R_s (s T_{sq} + 1)} \quad (4.15)$$

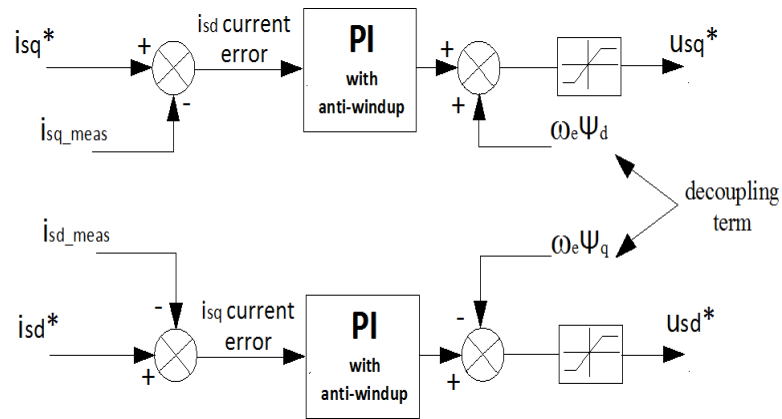


Figure 4.9 Current Coupling

Where:

$\tau_{sd} = \frac{L_d}{R_s}$ is the d electrical time constant.

$\tau_{sq} = \frac{L_q}{R_s}$ is the q electrical time constant.

4.3.1 Tuning the i_{sq} PI controller:

Here two method is used, the first one is the pole cancellation of the plant and use the system bandwidth and the second one is used mainly by the time delay of the system but as the simulation here MIL and the external device (ECU) is not used thus the system bandwidth is used for time delay and then they will be compare that which one of them have better performance with the

same bandwidth. In the **figure** the current loop is shown with taking into account the time delay and without time delay of the system.

4.3.1.1 Method one:

The Pi transfer function for speed loop is:

$$PI_q = K_p^q \frac{1+\tau_q s}{\tau_q s} = K_p^q + \frac{K_i^q}{s} \quad (4.16)$$

The open loop transfer function is the product of the PI controller and Plant transfer function.

$$G_q^{ol} = (K_p^q + \frac{K_i^q}{s}) (\frac{1}{s L_q + R_s}) \quad (4.17)$$

For close loop transfer function with unity feedback if the H is assume as G^{ol} , with use of general equation, the equation 4.18 is obtained.

$$G_q^{cl} = \frac{G_q^{ol}}{1+G_q^{ol}} \quad (4.18)$$

$$G_q^{cl} = \frac{(K_p^q + \frac{K_i^q}{s}) (\frac{1}{s L_q + R_s})}{1 + (K_p^q + \frac{K_i^q}{s}) (\frac{1}{s L_q + R_s})} \quad (4.19)$$

$$= \frac{K_p^q}{L_q} \frac{s + \frac{K_i^q}{K_p^q}}{s^2 + (\frac{R_s + K_i^q}{L_q})s + \frac{K_i^q}{L_q}}$$

The pole of the transfer function can be eliminated by electrical dynamic equation and use high bandwidth in the current loop. The upper limit frequency is the frequency of the SVPWM frequency that it is used. The bandwidth of the current loop must be at least one decade to the motor bandwidth. The bandwidth is equal to rad/s that is described more in detailed in the section. PI controller coefficient is earned by the calculation of the **equation 4.20**.

$$s^2 + \left(\frac{R_s + K_p^q}{L_q}\right)s + \frac{K_i^q}{L_q} = \left(s + \frac{K_i^q}{K_p^q}\right) + (s + \omega_c) \quad (4.20)$$

ω_c is the bandwidth of the current loop controller.

The equation can be written,

$$s^2 + \left(\frac{R_s + K_p^q}{L_q}\right)s + \frac{K_i^q}{L_q} = s^2 + \left(\omega_c + \frac{K_i^q}{K_p^q}\right)s + \omega_c \frac{K_i^q}{K_p^q} \quad (4.21)$$

And the PI controller coefficient for quadrature current control is earned by the using the equation 4.22.

$$K_p^q = \omega_c \cdot L_q \quad (4.22)$$

$$K_i^q = \frac{K_p^q (K_p^q + R_s)}{L_q} \quad (4.23)$$

Finally the PI coefficient for quadrature current controller are,

$$K_p^q = 1.9125 \quad K_i^q = 3.4125e+03$$

4.3.1.2 Method two

The PI controller tuning is done in continuous s domain. In real system the delay is taking into account. The delays are different according to the hardware devices that are used, they can be:

- Delay that cause by the digital calculation of the control algorithm, that it is equal to the inverse of frequency of the processor.
- Delay that cause by sampling that it is approximately.
- Delay that cause by the inverter switching and SVPWM modulation.

The Slowest pole of the BLDC motor is the one of the BLDC motor. The zero of the PI transfer function is set to cancel out this pole.

$$\tau_q = \frac{L_q}{R_s} = T_{sq} = 6.3034e - 04 \text{ Second} \quad (4.24)$$

For calculation of PI controller gain the time delay will be approximated as a time delay.

Open loop transfer function for i_q current controller by taking into account the time delay is:

$$G^{ol}_q = \frac{K_p^q}{\tau_q s} \frac{1}{R_s(T_{si}s+1)} \quad (4.25)$$

Calculation of T_{si} in calculated from bandwidth as the time delay here is not calculated due to the not using the external device and the just the time delay of MIL is consider that it is inverse of the desired bandwidth.

$$T_{si} = \frac{1}{\omega_c} \quad (4.26)$$

In the optimal modulus (OM) design method for design of PI gain controller for the q current controller damping factor of $\xi = \frac{\sqrt{2}}{2}$ is used [20]. Based on the OM method the generic open loop transfer function for a second order system is shown in formula 4.27.

$$G = \frac{1}{2\xi s(1+\xi s)} \quad (4.27)$$

By using this formula and compare it with open loop transfer function of i_{sq} current controller the following formula is obtained.

$$\frac{K_p^q}{R_s \tau_q} = \frac{1}{2T_{si}} \quad (4.28)$$

Therefore,

$$K_p^q = R_s \frac{\tau_q}{2T_{si}} = 0.956 \quad (4.29)$$

Thus of PI controller transfer function according to the calculated parameters is:

$$PI_\omega = 0.956 \frac{1+2.0000e-04 s}{2.0000e-04 s} = 0.956 + \frac{1.7063e+03}{s} \quad (4.30)$$

Thus PI controller parameters are:

$$K_p^q = 0.956$$

$$K_i^q = 1.7063e + 03$$

The bandwidth of the dynamic model of the motor is 1780.1 rad/s (283.3 Hz) and the bandwidth of current controller must be at least one decade more that the bandwidth of the dynamic model of the motor [23]. The bandwidth of 5000 rad/s (795.77 Hz).

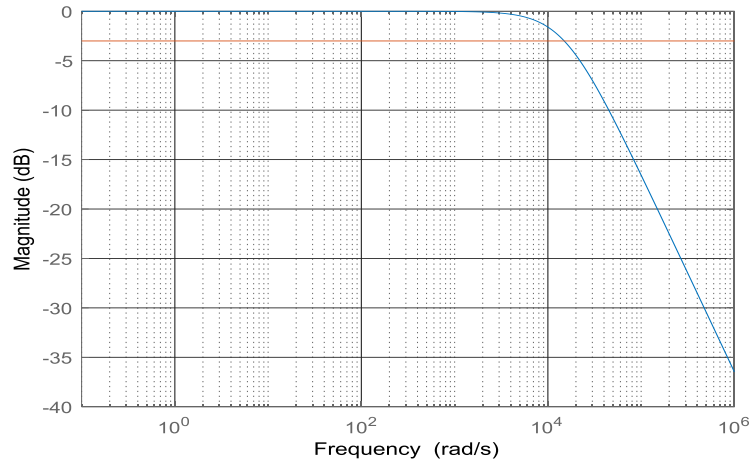


Figure 4.10 bandwidth

The close loop transfer function (CLTF) of the current control is,

$$G_{current}^{cl} = \frac{5000}{s+5000} \quad (4.31)$$

Bandwidth of CLTF at -3 db is 4988.1 rad/s that it is equal to 793.9 Hz. Sampling frequency of the ring must be:

$$f_s^{current} \geq 739.9 \text{ Hz}$$

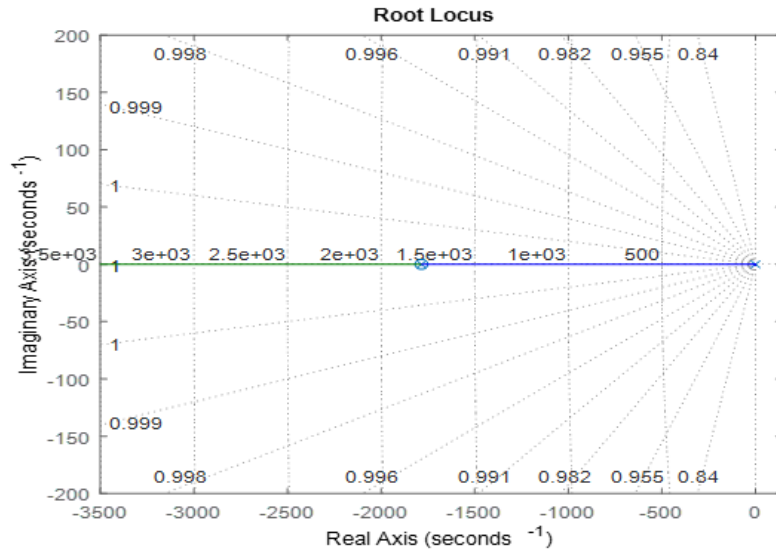


Figure 4.11 Root locus

The Bode diagram of the open loop transfer function is shown in figure 4.12.

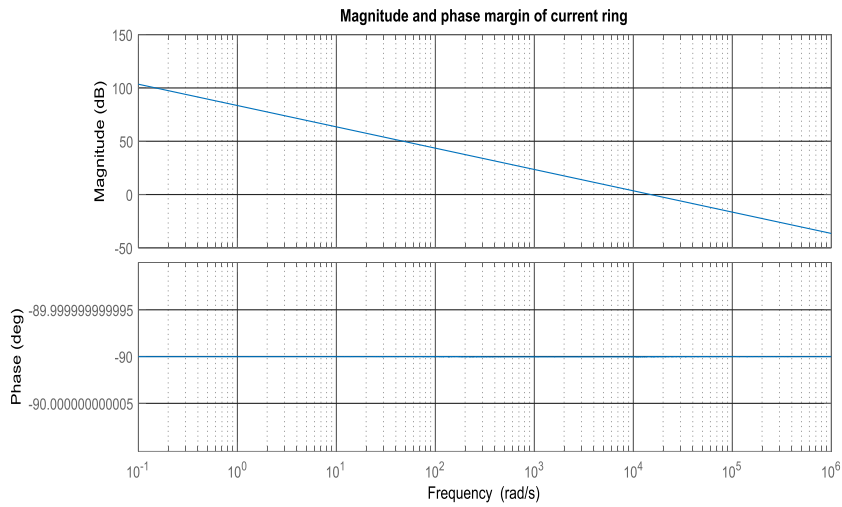


Figure 4.12 Bode plot diagram

According to the figure the i_{sq} closed loop system is stable.. The step response characteristic that also shown in the figure 4.13, are:

- Rise Time: 2.6080e-04
- Settling Time: 1.0000
- Settling Min: 0.9000
- Overshoot: 0
- Peak Time: 7.0306e-04

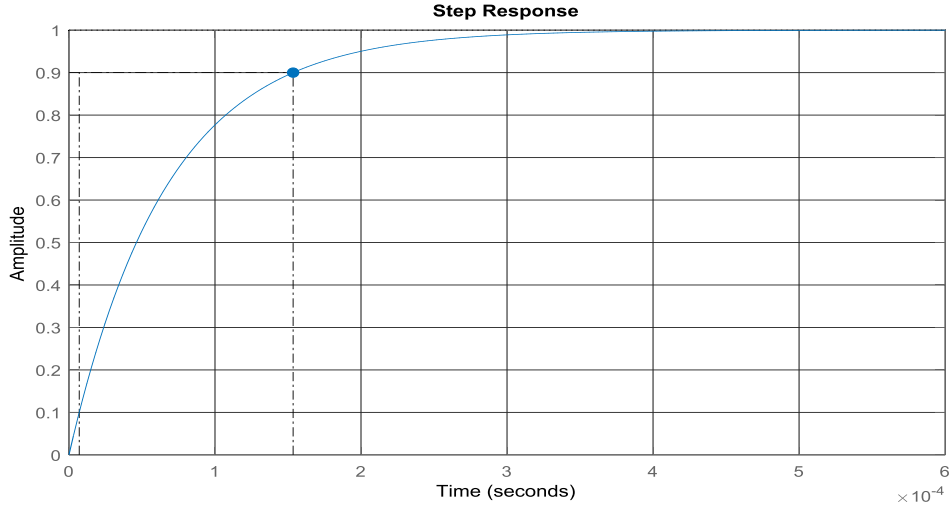


Figure 4.13 Step response

4.3.2 Tuning the i_{sd} PI controller

The open loop transfer function is the product of the PI controller and Plant transfer function.

$$G_d^{ol} = (K_p^d + \frac{K_i^d}{s}) (\frac{1}{s L_d + R_s}) \quad (4.32)$$

For close loop transfer function with unity feedback if the H is assume as G^{ol} , with use of general equation 4.33, the equation 4.34 is obtained.

$$G_d^{cl} = \frac{G_d^{ol}}{1 + G_d^{ol}} \quad (4.33)$$

$$G_d^{cl} = \frac{(K_p^d + \frac{K_i^d}{s}) (\frac{1}{s L_d + R_s})}{1 + (K_p^d + \frac{K_i^d}{s}) (\frac{1}{s L_d + R_s})} \quad (4.34)$$

$$= \frac{K_p^d}{L_d} \frac{s + \frac{K_i^d}{K_p^d}}{s^2 + (\frac{R_s + K_i^d}{L_d})s + \frac{K_i^d}{L_d}}$$

The pole of the transfer function 4.35, can be eliminated by electrical dynamic equation and use high bandwidth in the current loop. The upper limit frequency is the frequency of the SVPWM frequency that it is used. The bandwidth of the current loop must be at least one decade to the motor bandwidth.

PI controller coefficient is earned by the calculation of the equation 4.35.

$$s^2 + \left(\frac{R_s + K_i^d}{L_d}\right)s + \frac{K_i^d}{L_d} = \left(s + \frac{K_i^d}{K_p^d}\right) + (s + \omega_c) \quad (4.35)$$

ω_c is the bandwidth of the current loop controller.

The equation can be written,

$$s^2 + \left(\frac{R_s + K_p^d}{L_d}\right)s + \frac{K_i^d}{L_d} = s^2 + \left(\omega_c + \frac{K_i^d}{K_p^d}\right)s + \omega_c \frac{K_i^d}{K_p^d} \quad (4.36)$$

And the PI controller coefficient for quadrature current control is earned by the using the equation 4.37.

$$K_p^d = \omega_c \cdot L_d \quad (4.37)$$

$$K_i^d = \frac{K_p^d(K_p^d + R_s)}{L_d} \quad (4.38)$$

Finally the PI coefficient for quadrature current controller are,

$$K_p^d = 1.7212 \quad K_i^d = 3.4125e + 03$$

Method two

The PI controller tuning is done in continuous s domain. In real system the delay is taking into account. The delays are different according to the hardware devices that are used, they can be:

- Delay that cause by the digital calculation of the control algorithm, that it is equal to the inverse of frequency of the processor.
- Delay that cause by sampling that it is approximately.
- Delay that cause by the inverter switching and SVPWM modulation.

The Slowest pole of the BLDC motor is the one of the BLDC motor. The zero of the PI transfer function is set to cancel out this pole.

$$\tau_d = \frac{L_d}{R_s} = T_{sd} = 6.3034e - 04 \text{ Second} \quad (4.39)$$

For calculation of PI controller gain the time delay will be approximated as a time delay. Open loop transfer function for i_q current controller by taking into account the time delay is:

$$G^{ol}_d = \frac{K_p^d}{\tau_d s} \frac{1}{R_s(T_{si}s + 1)} \quad (4.40)$$

Calculation of T_{si} in calculated from bandwidth as the time delay here is not calculated due to the not using the external device and the just the time delay of MIL is consider that it is inverse of the desired bandwidth.

$$T_{si} = \frac{1}{\omega_c} \quad (4.41)$$

In the optimal modulus (OM) design method for design of PI gain controller for the q current controller damping factor of $\xi = \frac{\sqrt{2}}{2}$ is used [20]. Based on the OM method the generic open loop transfer function for a second order system is shown in formula 4.42.

$$G = \frac{1}{2\xi s(1 + \xi s)} \quad (4.42)$$

By using this formula and compare it with open loop transfer function of i_{sq} current controller the following formula is obtained.

$$\frac{K_p^d}{R_s \tau_d} = \frac{1}{2T_{si}} \quad (4.43)$$

Therefore,

$$K_p^d = R_s \frac{\tau_q}{2T_{si}} = 0.8606 \quad (4.44)$$

Thus of PI controller transfer function according to the calculated parameters is:

$$PI_\omega = 0.8606 \frac{1+2.0000e-04 s}{2.0000e-04 s} = 0.8606 + \frac{1.7063e+03}{s} \quad (4.45)$$

Thus PI controller parameters are:

$$K_p^d = 0.8606 \quad K_i^d = 1.7063e + 03$$

The bandwidth of the dynamic model of the motor is 1780.1 rad/s (283.3 Hz) and the bandwidth of current controller must be at least one decade more that the bandwidth of the dynamic model of the motor [23]. The bandwidth of 5000 rad/s (795.77 Hz).

The close loop transfer function (CLTF) of the current control is,

$$G_{current}^{cl} = \frac{5000}{s+5000} \quad (4.46)$$

Bandwidth of CLTF at -3 db is 4988.1 rad/s that it is equal to 793.9 Hz. Sampling frequency of the ring must be:

$$f_s^{current} \geq 739.9 \text{ Hz}$$

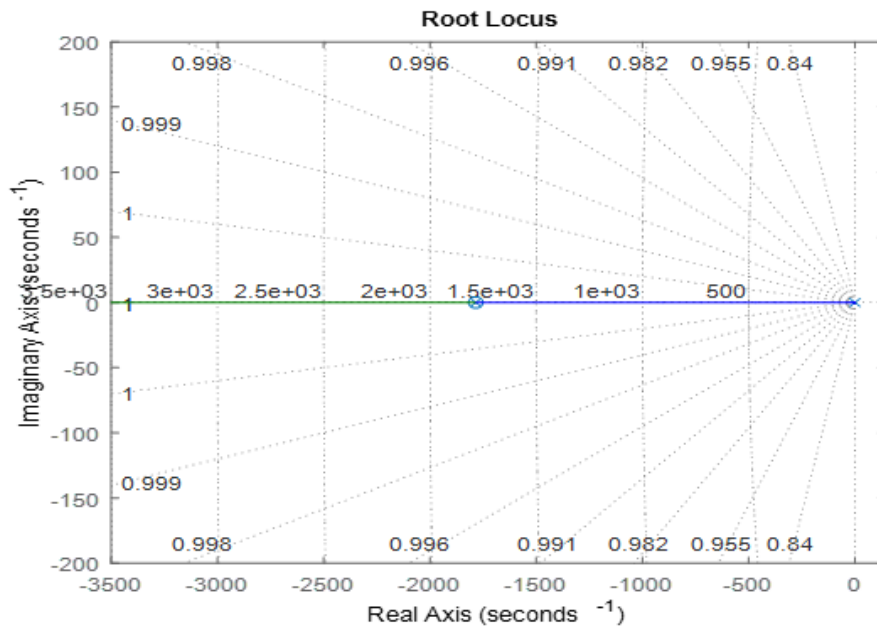


Figure 4.14 Root locus

The Bode diagram of the open loop transfer function is shown in figure. In the first method one real pole exist and the system is stable. And the margin is 90° because of existence of the integrator.

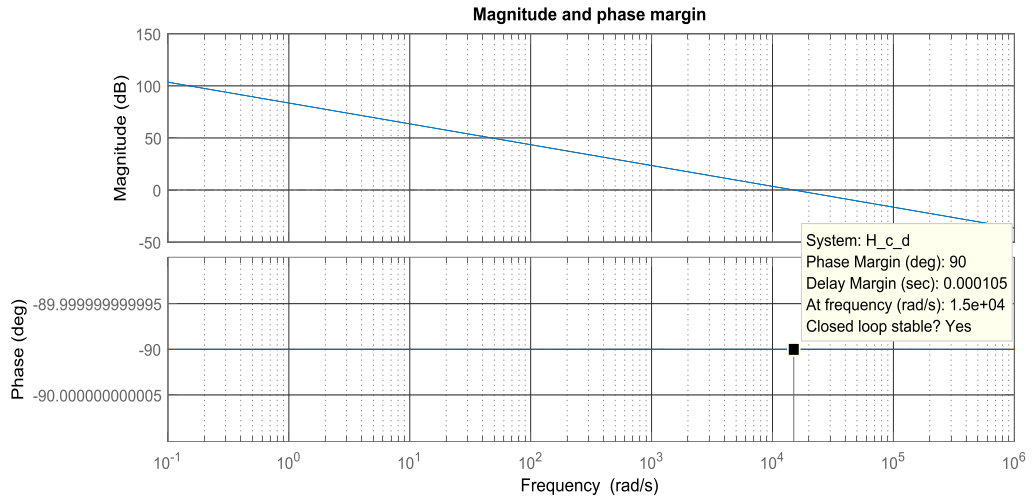


Figure 4.15

According to the figure the i_{sq} closed loop system is stable.. The step response characteristic that also shown in the figure 4.16, are:

- Rise Time: 1.4647e-04
- Settling Time: 2.6080e-04
- Settling Max: 1
- Settling Min: 0.9000
- Overshoot: 0
- Peak Time: 7.0306e-04

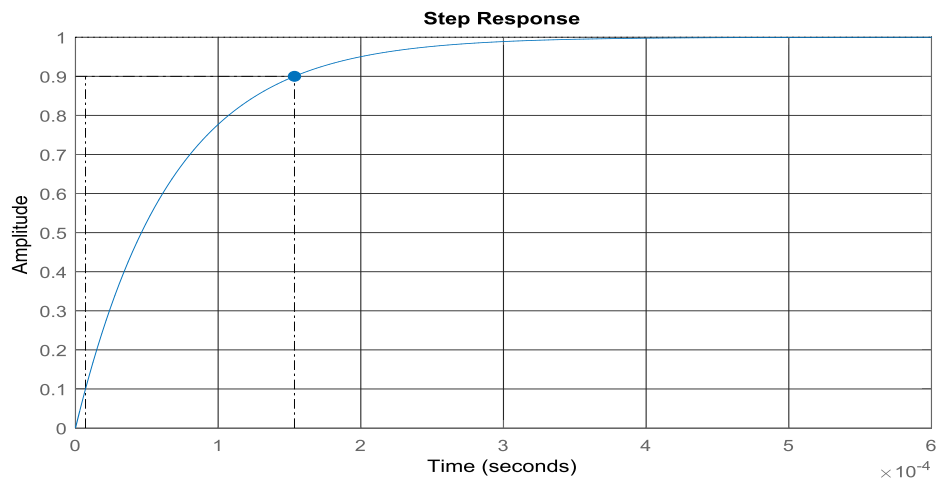


Figure 4.16 Step response

4.3 Speed control

Speed controller block is added to the outer loop of FOC. Input parameter to the speed control block is the error signal that produce by the mechanical reference speed and measured mechanical speed. The output of the speed control block is T^* torque that the torque convert to i^*_q and i^*_d by MTPA (maximum torque per ampere) term which will explain later.

Open loop transfer function of speed controller calculated and it is,

$$G_{speed}^{ol} = (K_p^w + \frac{K_i^w}{s}) \cdot (\frac{B_c}{s+B_c}) \cdot (\frac{3}{2} K_t \cdot n_p) \cdot (\frac{1}{b_{mot}} \cdot \frac{1}{1+\frac{J_{mot}}{b_{mot}}s}) \quad (4.47)$$

Then, the CLTF of the speed with unity feedback is:

$$G_w^{cl} = \frac{(\frac{K_p^w + K_i^w}{s}) \cdot (\frac{B_c}{s+B_c}) \cdot (\frac{3}{2} K_t \cdot n_p) \cdot (\frac{1}{b_{mot}} \cdot \frac{1}{1+\frac{J_{mot}}{b_{mot}}s})}{1 + (\frac{K_p^w + K_i^w}{s}) \cdot (\frac{B_c}{s+B_c}) \cdot (\frac{3}{2} K_t \cdot n_p) \cdot (\frac{1}{b_{mot}} \cdot \frac{1}{1+\frac{J_{mot}}{b_{mot}}s})} \quad (4.48)$$

Finally the speed PI controller coefficient are:

$$K_i^w = K_p^w (B_c + \frac{b_{mot}}{J_{mot}} - 2 \cdot B_w) \quad (4.49)$$

$$K_i^w = \frac{K_p^w (B_c \cdot b_{mot} + K_p^w \cdot \frac{3}{2} K_t \cdot n_p \cdot B_c)}{2J_{mot} \cdot B_w} - \frac{K_p^w}{2}$$

$$K_p^w = \frac{B_w^2 \cdot J_{mot}}{c \cdot B_c} \quad (4.50)$$

In order to have a stable system we need a positive K_i^w :

$$B_w \leq \frac{1}{2} \cdot (B_c + \frac{b_{mot}}{J_{mot}}) \quad (4.51)$$

And finally the bandwidth of the speed loop is set to 2500 rad/s () and the speed PI control results are:

$$K_i^w = 0.0211 \quad K_p^w = 0$$

The bandwidth at -3 db is 4817.2 rad/s (766.68 Hz), and the sampling frequency of the loop must be:

$$f_s^{speed} \geq \text{Bandwidth (Hz)} \quad (4.52)$$

$$f_s^{speed} \geq 1533.4 \text{ Hz}$$

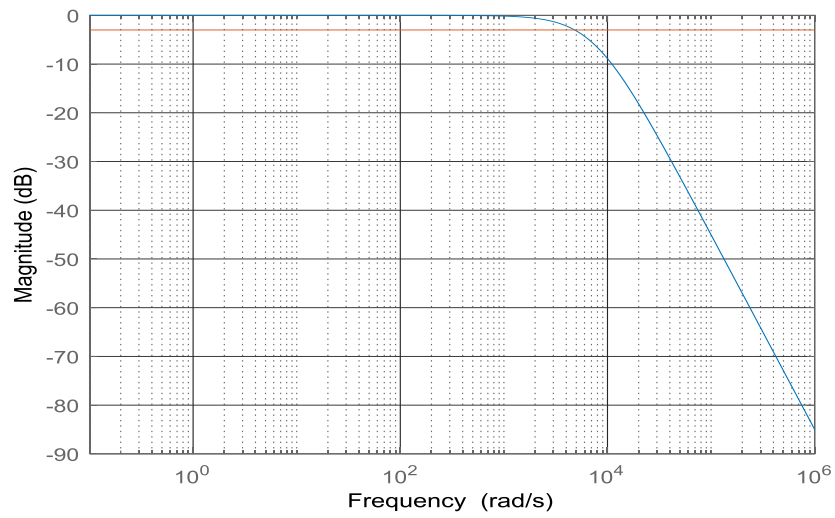


Figure 4.17 Bandwidth

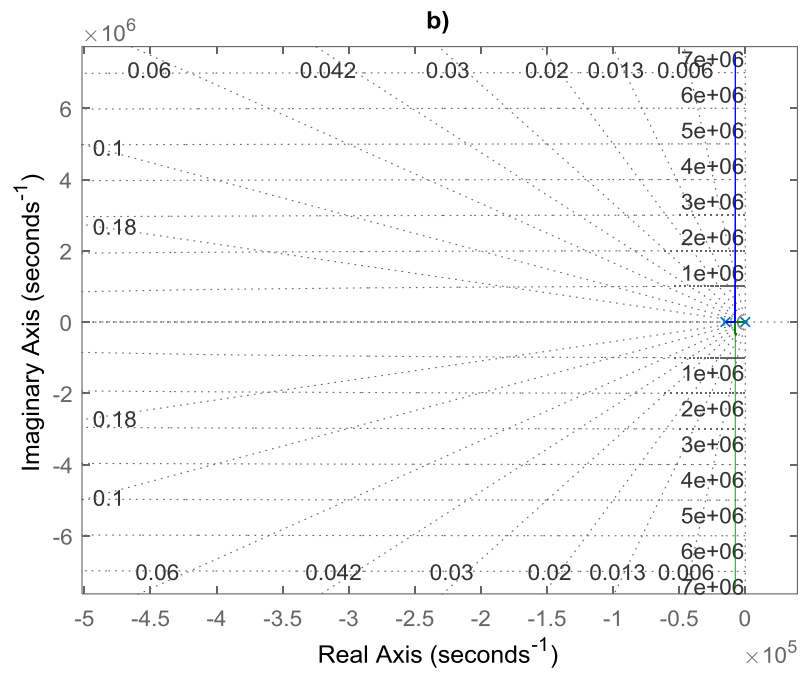


Figure 4.18 Root locus

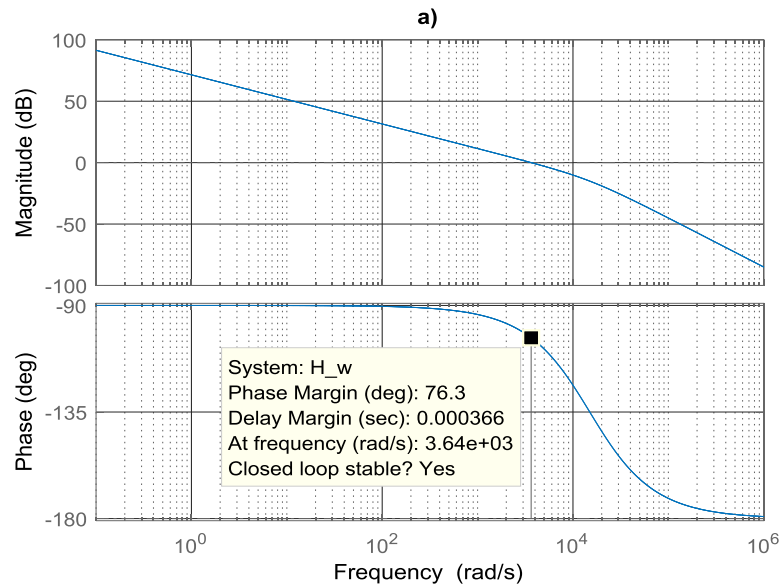


Figure 4.19 bode plot diagram

4.4 Anti-windup for Current loop controller

Anti-windup is used to avoid saturation of the controller during the saturation. Here the back-calculation anti-windup is used as the difference between saturated and unsaturated control signal is used as feedback signal to proper control. Then the feedback signal is multiply by a gain that it is called anti-windup gain. By increasing the anti-windup gain the integrator can be limited quickly, but very high gain may cause a big error, which cause the PI controller to reset. Normally the anti-windup gain is inverse of proportional gain [21]. The anti-windup gain is selected experimentally by running the simulation.

The output of the current control is the voltage and the voltage outputs of the current controller have a limitation, this limitation is according to the DC link voltage of the inverter that here, it is 18V. Anti-windup is used to prevent the saturation of the dq reference voltage in the output of the current controller. The diagram of the current controller with anti-windup is shown in figure.

In speed controller by the torque output of the speed loop the direct and quadrature currents are calculated and then these current are used also for anti-windup of the speed controller.

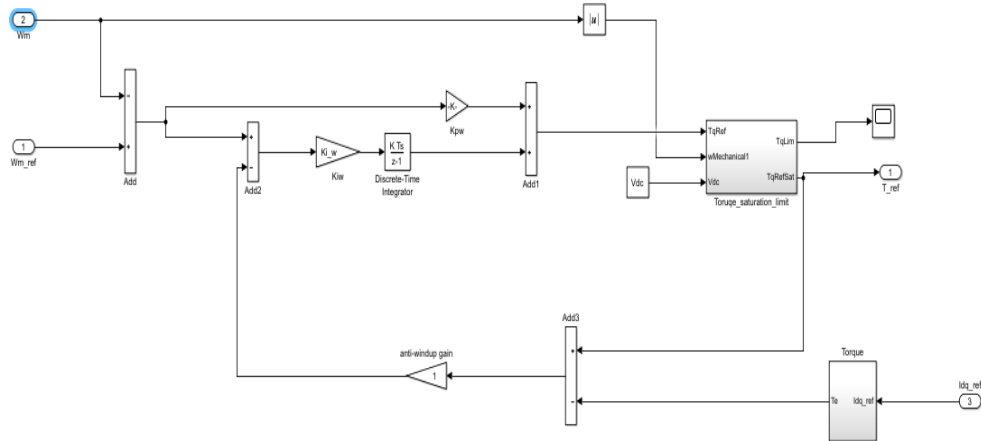


Figure 4.20 Anti-windup in speed control

4.5 Maximum Torque per Ampere (MTPA)

The copper losses are depend to the stator current. With stator current increase also the copper loss increase; also stator control increase with increase of the torque. MTPA is used to use the minimum current for the desired torque that it cause the copper loss in the motor. In reality it is not only the q-axis that produce torque, but also the d-axis produce torque that it is called reluctance torque [20].

The motor parameters change due to the load and temperature during the running process of the pump, the most change come to parameters L_q , L_d and Ψ_m , that they also have affect to the MTPA. In **figure**, the variation of current vector angle β and torque T_e are shown, The β_{MTPA} is the curve tangent point of the constant torque. And by changing the position of the angle β , the derivative value increase or decrease from zero. The motor is operating on the optimal point of MTPA can be confirmed though detecting that whether the value of the $dT_e/d\beta$ is zero [23]. Here in this thesis the rate of change of these parameters due to the temperature and load change is not considered.

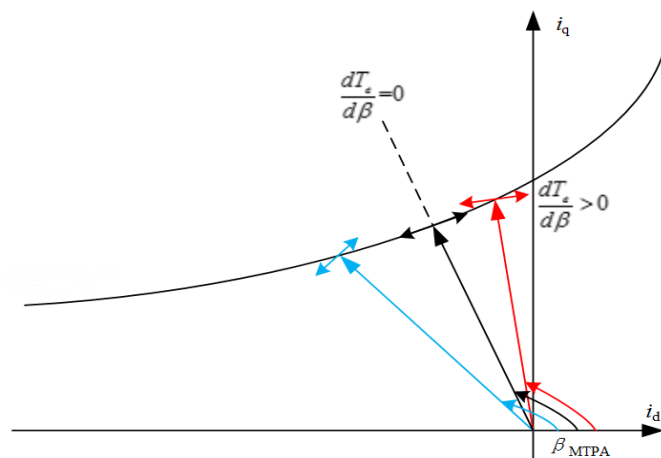


Figure 4.21 MPTA curve

The MTPA curve is earned by the electro-magnetic torque equation.

$$T_e = \frac{3}{2}p_b(\Psi_m i_{sq}) + \frac{3}{2}p_b(L_d - L_q)i_{sq}i_{isd} \quad (4.65)$$

The current limit of MTPA is the available output of the inverter that in the reality also depend to the thermal dissipation, and other characteristic of the inverter that effect the inverter output current.

$$\sqrt{i_d^2 + i_q^2} = i_s \leq i_{max} \quad (4.66)$$

The current limit constraint form circle shape with a center position at the origin with radius that it names i_{max} .

$$T_e = \frac{3}{2}p_b(\Psi_m \sqrt{i_{sq}^2 + i_{sd}^2} + (L_d - L_q)i_{sd} \sqrt{i_{max}^2 - i_{sd}^2}) \quad (4.67)$$

From [equation](#) the following equation is driven [18].

$$\frac{dT_{mech}}{di_{sd}} = \frac{3}{2}p_b \cdot \frac{-i_{sd}\Psi_m + (L_d - L_q)(I_{max} - 2i_{sd}^2)}{\sqrt{I_{max}^2 - i_{sd}^2}} \quad (4.68)$$

Then,

$$2i_{sd}^2 + \frac{\Psi_m}{L_d - L_q}i_{sd} - I_{max}^2 = 0 \quad (4.69)$$

Minimum quadrature current formula is,

$$i_{sd} = \frac{\sqrt{\Psi_m^2 + 8(L_d - L_q)^2 I_{max}^2} - \Psi_m}{4(L_d - L_q)} \quad (4.70)$$

For calculation of MTPA the parameters of BLDC motor from [table](#) is used. The MTPA is calculated from zero to the maximum range of current that it the inverter current limit (I_{max}); the other parameter, as it is said before, they are constant. The calculated values are implemented into two lookup tables, one for i_d derivation and the other for i_q derivation [18]. The lookup table do the form of these function $i_d = f(T_e)$ and $i_q = f(T_e)$, it take the torque as input and provide the reference currents i_d and i_q as output. The Simulink block of the MTPA is shown in [figure](#).

4.6 Field Weakening

The voltage and current of motor are limited to maximum voltage and current of inverter, the limited voltage and current are represented in equation 4.71. With respect to the maximum inverter voltage and hence maximum input machine voltage and rated torque, the machine attains to the rated speed. The back-emf is limited by the applied voltage to the motor, when the back-emf limit is reached the motor speed can't increase to the back-emf limit. The flux weakening is proportional to the stator frequency so that the induced back-emf is a constant and will not increase with increasing speed [12]. In the field weakening the rotor flux is not change, all thing that it is done is decreasing of rotor flux that couple into the stator coil that it is cause Back-EMF that we want decrease.

$$V_d^2 + V_q^2 \leq V_{max}^2 \quad (4.71)$$

$$i_d^2 + i_q^2 \leq i_{max}^2 \quad (4.72)$$

The voltage equation by the use of dq dynamic voltage equation and dq flux equation can be written in the following form.

$$V_d = R_s i_d + L_d \frac{di_d}{dt} - \omega_e L_q i_q \quad (4.73)$$

$$V_q = R_s i_q + L_q \frac{di_q}{dt} - \omega_e L_d i_d + \omega_r \Psi_f \quad (4.74)$$

The voltage constraint can be written in terms of currents under assumption of steady state operation or slow enough variation of current by using equation 4.75 [24].

$$Z_d^2 \left(i_d + \frac{\omega_e^2 L_q \Psi_f}{R_s^2 + \omega_s^2 L_d L_q} \right)^2 + Z_q^2 \left(i_q + \frac{\omega_e^2 L_q \Psi_f}{R_s^2 + \omega_s^2 L_d L_q} \right)^2 + 2\omega_e R_s (L_d - L_q) \left(i_d + \frac{\omega_e^2 L_q \Psi_f}{R_s^2 + \omega_s^2 L_d L_q} \right) \left(i_q + \frac{\omega_e L_q}{R_s^2 + \omega_s^2 L_d L_q} \right)^2 \leq V_{max}^2 \quad (4.75)$$

The above equation is when parameters of motor L_d and L_q their values are different. But when L_d and L_q are equal the following equation is derived.

$$\left(i_d + \frac{\omega_e^2 L_q \Psi_f}{R_s^2 + \omega_s^2 L_d L_q} \right)^2 + \left(i_q + \frac{\omega_e R_s}{R_s^2 + \omega_s^2 L_d L_q} \right)^2 \leq \frac{V_{max}^2}{R_s^2 + (\omega_e L_s)^2} \quad (4.76)$$

By using the equation 4.76, when the L_d and L_q have different values, it represent an ellipse that shown in figure. And equation 4.77, when the L_d and L_q have the same values, it represent a circle that shown in figure 4.22. The center of ellipse is earn by the following formula:

$$I_{inf} = \frac{-\Psi_m}{L_d} \quad (4.77)$$

By increasing of speed the ellipse area decrease and the center of the ellipse reach at infinite speed, as shown in figure the center of ellipse is located outside of current limit circle that it show that the infinite speed point is not reachable due to the maximum current limit. Sometimes the center of ellipse is located inside ellipse, in this situation it is needed to use voltage limitation also.

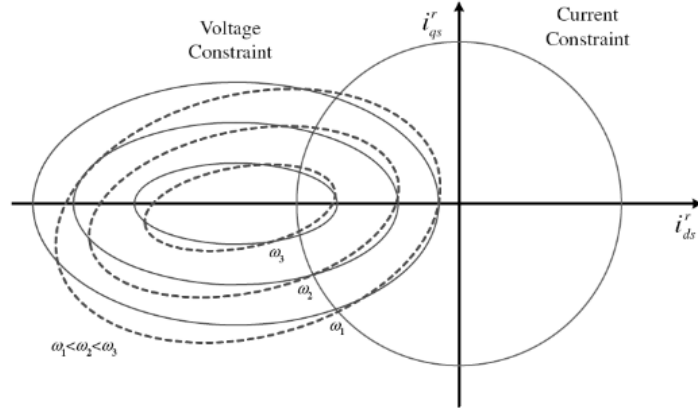


Figure 4.22 Voltage limit with difference values of inductances

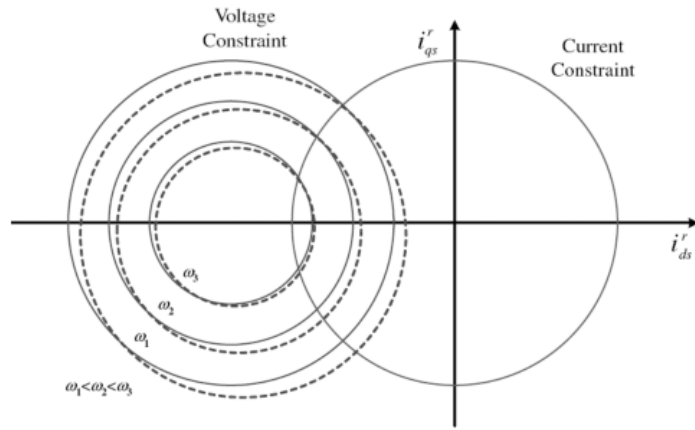


Figure 4.23 Voltage limit with equal inductance parameters

The maximum possible operating speed of sinusoidal BLDC motor with neglecting the stator resistance is [24]:

$$\omega_c = \frac{V_{max}}{\sqrt{(L_s I_{max})^2 - \Psi_f^2}} \quad (4.78)$$

The field weakening model that it is used here, it is from Simulink block. It is a parameter-insensitive that means the motor parameters are not into account in this model. The operation mode is that when reference voltage exceed limit voltage (maximum voltage of inverter that can operate) then the field weakening start its work. As shown in figure , for implementation of field weakening first the references current $i_{d,ref}$ and $i_{q,ref}$ are converted to polar from Cartesian and after the operation is done then it polar convert to polar. Modulation is used for activation of field weakening when it is needed. The modulation input are measured direct voltage ($u_{d,meas}$) and quadrature voltage ($u_{q,meas}$) and voltage limit of inverter (U_{dc}). By using the input values and using the equation the modulation index is calculated.

$$M = \frac{\sqrt{u_{d,meas}^2 + u_{q,meas}^2}}{U_{dc}} \quad (4.79)$$

The algorithm that it is used, reducing the angle of commanded current with respect to the d-axis current, it is shown in figure.

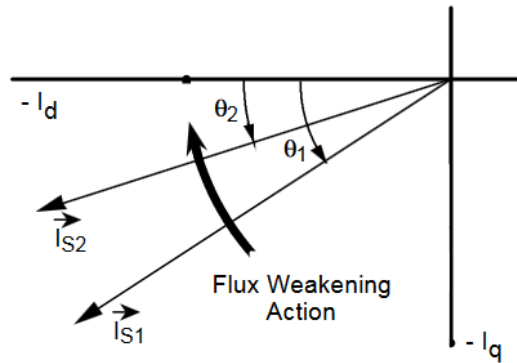


Figure 4.24 Directive current performance in field weakening

After modulation index a PI controller with anti-windup is used, this controller is named β and its value is between zero and one. When value of β is one, the flux weakening control module exerts no influence on the current vector trajectory. Threshold level is indicated by M_{th} , its value is less than but close to one. Any value of M above the threshold level cause reduction in β value, that the new angle value is $\vartheta = \beta \cdot \vartheta$ [25].

When the speed and torque decrease and come down the base value, the feedback loop cause reduction of its effect on vector angle ϑ . That cause the value β goes back to one when the modulation index drop below the threshold level. Using V_{dc} make suitable control with change of voltage that in automotive depend on state of charge of battery (SOC) and battery load [25].

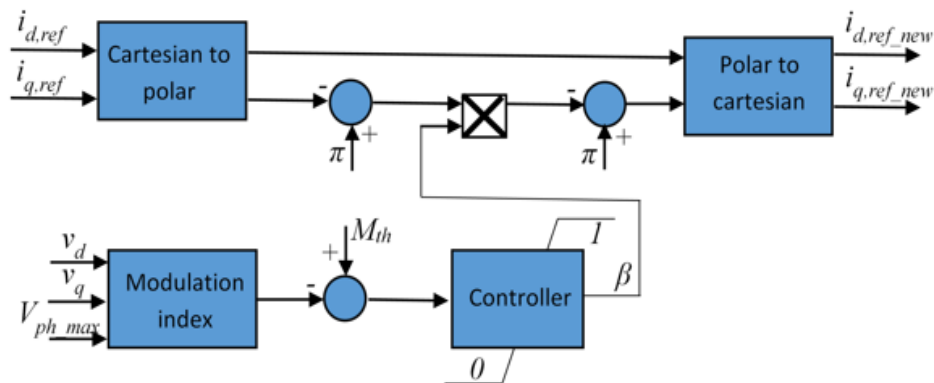


Figure 4.25 Field weakening operation

Algorithm for Hydraulic Control

In this chapter the control of fluid with respect to the electrical motor performance is done. An introduction to fuel pressure in cars is described. Also overall view to fuel pump structure is described. Battery state charge of changing is automotive is discussed. And finally some safety operation in and overall control view automotive of fuel pump is described.

5.1 Pressure control

Pump performance have direct relation with electrical motor speed. For earning the desired speed of the motor to supply the desired pressure a control feedback form the fluid characteristic to the motor is needed. As it is described in chapter two, the fuel pressure is measured by the pressure sensor, also the desired pressure need of engine is the goal that must be achieved.

An error signal that is the result of the differences between the desired pressure and measured pressure is calculated instantly. The pressure error has to multiply by a gain to faster achieve the desired performance in loop operation. The error signal is multiply by 100.55, that it is the pressure vs. motor speed ratio (at pressure of 36 psi with 3620 rpm), then result of this procedure is added to the speed reference of 6320 rpm. The 6320 rpm speed reference is used in order to earn the desired speed, when the pressure error signal is zero the speed reference is 6320 rpm, and when the measured pressure is different from the desired pressure the final reference is below or above 6320 rpm speed. The feedback control structure is shown in figure 5.1.

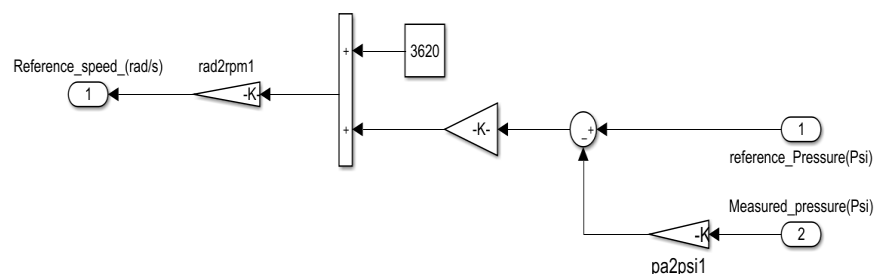


Figure 5.1 Feedback control structure

5.2 Fuel Pressure

Fuel pressure has a direct effect on engine operation. Volume and pressure have reciprocal relation together, highest volume occur when there is free flow of fuel and there is no pressure, also for highest pressure it is vice versa. Each engine require different fuel pressure. For example a carbureted engine typically require 4 to 7 psi whereas a typical GM LS engine runs around 58 psi. In table 5.1, some pump pressure of Airtex fuel pump is shown, there are a lot of different fuel pump.

Carbureted Applications

PART NUMBER	VOLTS	PRESSURE	FLOW	INLET/OUTLET SIZE	SUGGESTED APPLICATIONS	Gasoline	Diesel
E8004	12	4–6 PSI	35 GPH	5/16" Hose	High Performance Carbureted Applications	✓	✗
E8011	6	5–8 PSI	30 GPH	5/16" Hose	6 Volt Carbureted Applications	✓	✓
E8012S	12	5–9 PSI	30 GPH	5/16" Hose	Domestic Carbureted, 5/16" hose	✓	✓
E8016S	12	2.5–4.5 PSI	30 GPH	5/16" Hose	Import Passenger and Light Truck Carb	✓	✓
E8090	12	5–9 PSI	30 GPH	3/8" Hose	Domestic Carbureted, 3/8" hose	✓	✓
E8135	24	5.5–9 PSI	35 GPH	3/8" Hose	Large Carbureted Gas Engines, 24 volt system	✓	✓
E8902	6	2.5–4.5 PSI	30 GPH	5/16" Hose	6 Volt Carbureted Applications	✓	✓

Fuel-Injected Applications

PART NUMBER	VOLTS	PRESSURE	FLOW	INLET/OUTLET SIZE	SUGGESTED APPLICATIONS	Gasoline	Diesel
E8094	12	12–17 PSI	45–50 GPH	5/16" Hose	GM TBI Replacement	✓	✗
E8228	12	100–125 PSI	38 GPH	5/16" Hose	MPI Universal Replacement	✓	✗
E8248	12	110–120 PSI	60–70 GPH	3/8" Hose	High Performance MPI	✓	✗
E8445	12	45–65 PSI	35 GPH	5/16" Hose	Universal Fuel Injection Pump	✓	✗
E8446	12	105–115 PSI	50–60 GPH	5/16" Hose	Universal Fuel Injection Pump	✓	✗

Table 5.1 Fuel pressure of some automotive fuel pump

5.3 Fuel pump structure:

The fuel insert to the inlet port of the fuel, after the pressure and velocity is added by the vanes to the fluid. Then it cross from surrounding of electrical motor and then it goes through the exit port. In figure 5.2, the complete structure of fuel pump is shown, it is Bosch fuel pump. The figure detail that shewn each part of pump are:

- Electrical connection
- Hydraulic connection (fuel outlet)
- Non-return valve
- Carbon brushes
- Motor armature with permanent magnet
- Impeller
- Hydraulic connection (fuel inlet)

Electrical connection is used for connection of DC voltage (battery voltage) to the pump. Non-return valve is used to avoiding fuel flow back to the pump. Fuel inlet is the fuel flow to the pump and the fuel outlet is the exit port of the fuel.

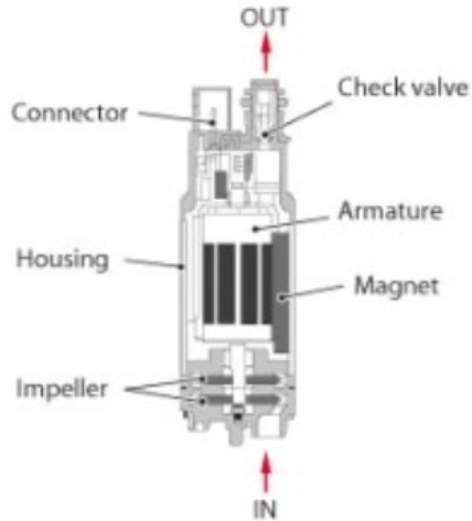


Figure 5.2 Electrical fuel pump structure

5.4 Battery

Battery is a device that convert chemical energy to electrical energy and vice versa. State of Charge (SoC) show fuel gauge for battery pack in vehicle. The unit of SoC is in percentage, for empty battery, it is zero percent and for full charge, it is 100%. Usually, SoC cannot be measured directly, but it can be estimated from direct measurement variable in online and offline ways.

Here our focus is not to calculate the SoC. SoC normally is used when discussing the current state of battery. Voltage is more affected by battery current and temperature []. The important part is that battery voltage change is changing with SoC variation and it have effect in (electrical motor of) fuel pump. Here our concern is to discuss the result of this voltage variation performance of the fuel pump.

In figure 5.2, the voltage variation of battery from zero percent to 100% SoC at 25 °C is shown. The voltage range between 12.24 V to 12.73 V is good voltage condition of the battery. The voltage from 11.96 V to 12.10 V is the zone that not recommended. And the SoC charge between zero percent to 30% must be avoided because it decrease battery life.

No Load voltage reading	% Charge
12.73	100%
12.62	90%
12.50	80%
12.37	70%
12.24	60%
12.10	50%
11.96	40%
11.81	30%
11.66	20%
11.51	10%
10.50	0%

Figure 5.3 Battery state of charge

5.5 Safety function

As it described in previous chapters, the motor of fuel pump is cooled by the fuel when the fuel is pumped, because of fuel crossing from surrounding of electric motor. If motor work when there is no fuel in tank of vehicle may cause of temperature rising and electrical motor fault. For avoiding such kind of failure a is installed on in-tank fuel pump kit, and for in-line fuel pump there is the possibility of installing a sensor for detecting fuel level in tank.

This safety algorithm must work in a way that with fuel level reduction from a limit, it stop the operation of fuel pump to avoid electrical motor damage. The Simulink model of this operation is shown in figure 5.3. Also, the other benefit of sensor is to show the fuel level to the driver that driver can go to fuel station early. Filter is used through the inlet pipe of the pump to detect the solid material in the pump that is one the most relevant reason of pump fault.

When the pump cannot deliver the right amount of the fuel pressure and volume, the engine experiences lean misfires. Because there not enough amount fuel for combustion. Lean Misfires cause the rise of engine temperature due to the engine operation hotter that the normal operation.

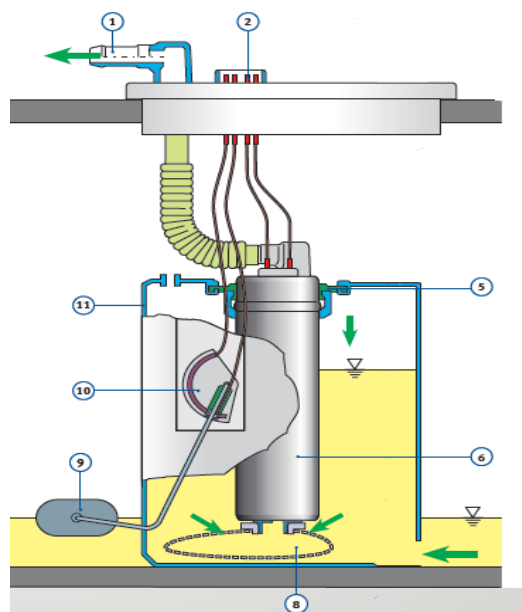
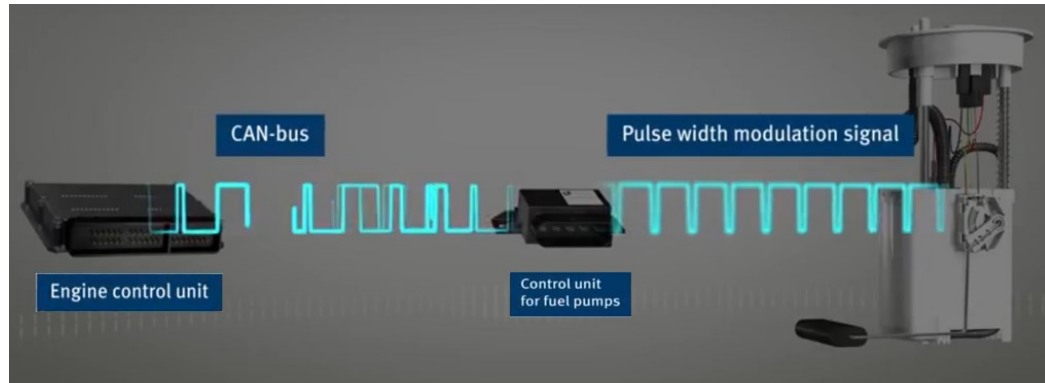


Figure 5.3 In-tank fuel pump kit

5.6 Control unit

Control algorithm of fuel pump is implemented in the ECU for fuel pump. The output of ECU for fuel pump is a PWM signal that control the operation inverter that deliver electricity to electorator motor. Also the data of fuel level sensor transmit to the ECU for fuel pump. Then the data of fuel level sensor from the ECU and also fuel pump operation condition can transfer to the pump that control algorithm operate in a good condition for safety or maybe for other reason. Also, engine control unit transfer the value of required pressure that needed for fuel system, also engine control unit may command to stop the fuel pump in critical condition like accident.



Evaluation of Simulation Result

The previous chapters discuss about the modeling and simulation electric motor using FOC, other control peripheral method with FOC, like MTPA and field oriented control, hydraulic pressure control and some other safety characteristic that take into account of fault avoidance in operation of automotive fuel pump. In this chapter the result of these simulation is shown and discussed.

6.1 Electrical motor general characteristic

The speed result of motor is important part because it is the main part of fuel pump control. The threshold of the speed with reference speed that requested from motor are the key point of electrical motor results. In the following figure the speed tracing of motor with respect to reference speed and its resonance is shown in figure 6.1. The motor speed reaches the reference speed at 0.07 second.

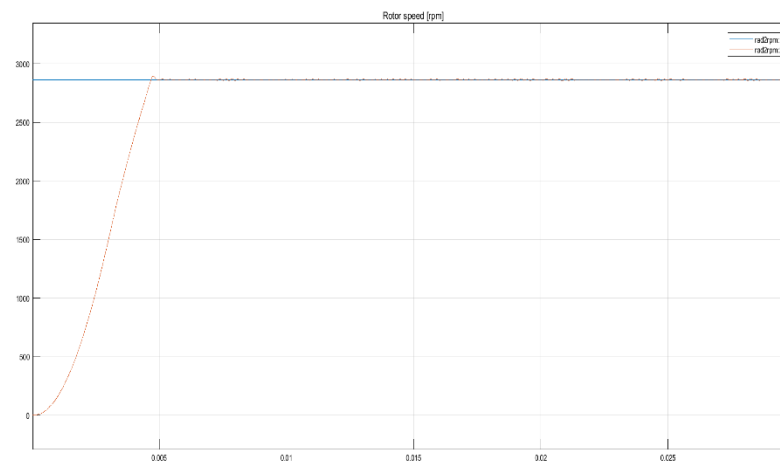


Figure 6.1 Motor speed with the reference speed

Change in speed cause torque variation, in figure 6.3, the result of increasing in speed of electrical motor cause overshoot in the torque result of the motor.

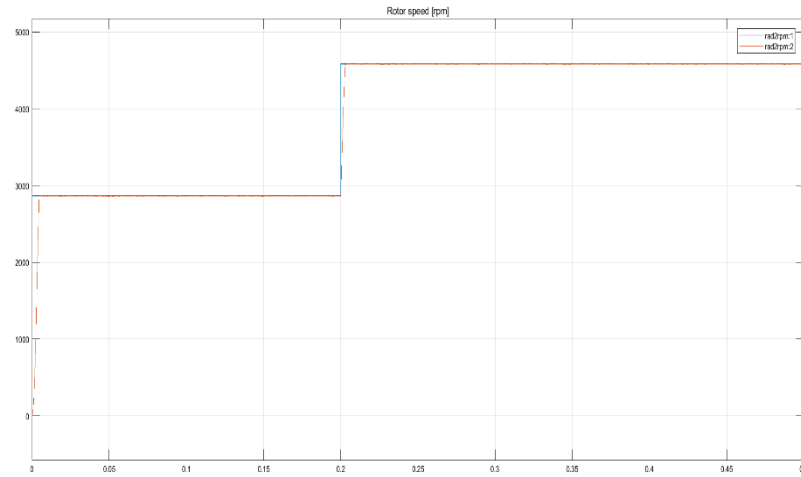


Figure 6.2 Motor speed operation with change of reference speed

Also, the speed variation cause the change in stator current of the motor, in the following figure the result of speed variation cause and increase of current until the motor reach the desired speed value.

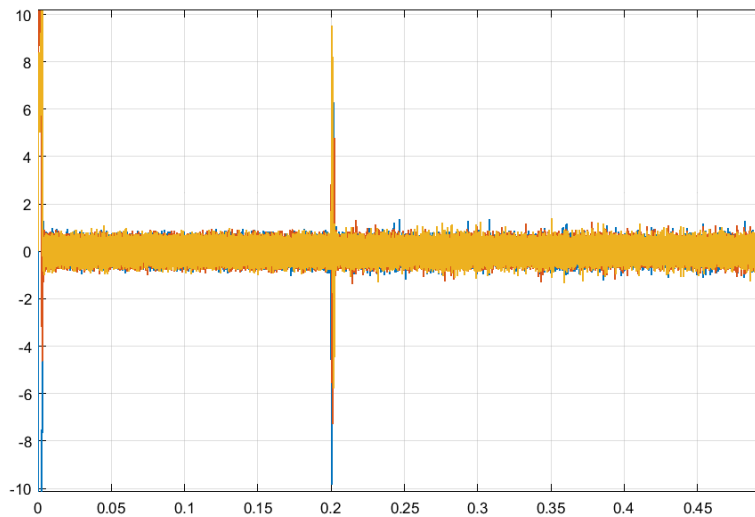


Figure 6.3 Motor stator current with change of motor speed

Motor speed decrease with operation of fuel pump, due to the increasing of the torque with respect to the increasing of load, it has direct effect on the speed of the motor. The motor speed decrease with increasing of torque. In the simulation the torque of the pump is connected to the motor and thus the torque have direct effect on the speed of the motor. The motor speed with during the operation of the pump with 0.2 (Nm) torque is shown in the figure 6.5. As it is shown in the figure, the motor speed decreased due the high torque of the fuel pump.

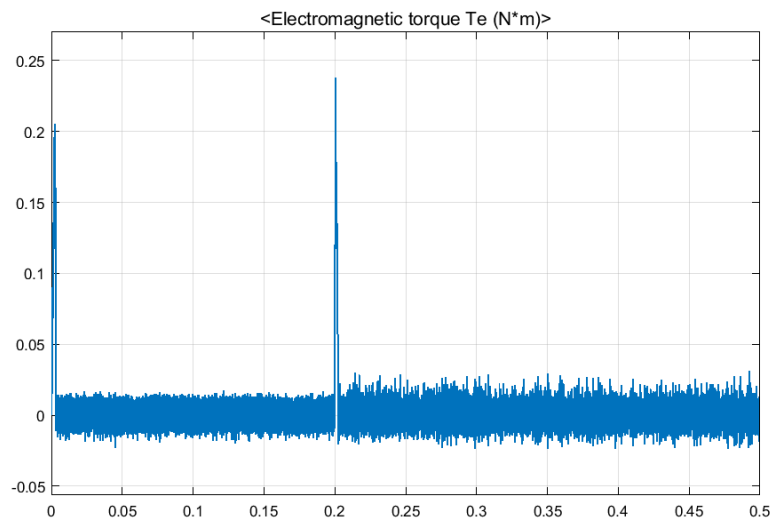


Figure 6.4 Motor electromagnetic torque

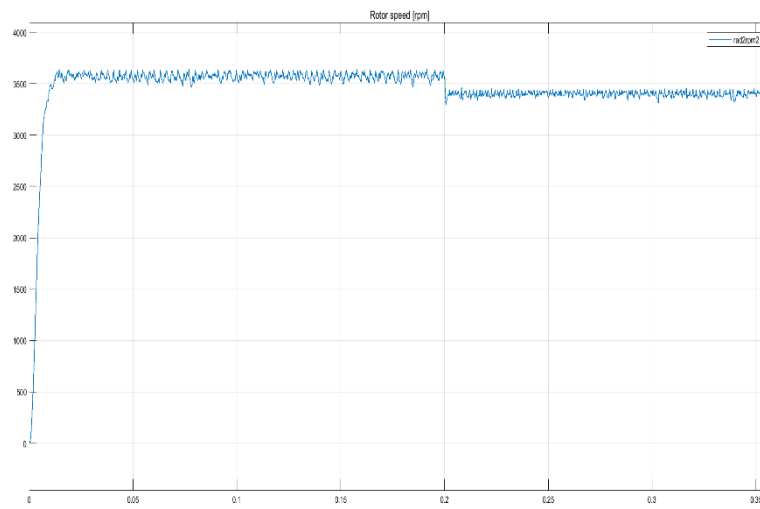


Figure 6.5 Motor speed during the pump operation

6.2 Hydraulic characteristic

The desired pressure for the electrical pump is assumed as 36 psi, also during the simulation the change of desired pressure is take into consideration. In figure 6.6, the pressure of the pump is shown. The pump follow the desired pressure, but there are ripples in the pressure.

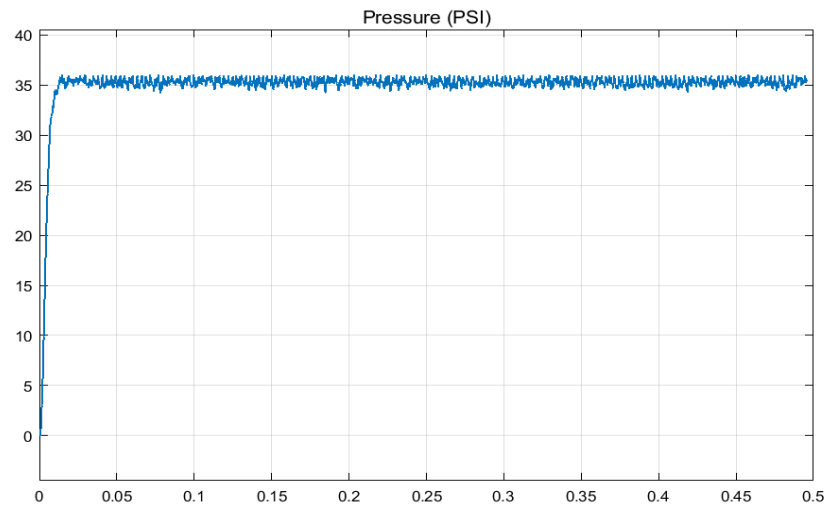


Figure 6.6 Pressure of the pump psi unit

Here, in figure the change of pressure from 36 psi to 32 psi in time of 0.2 seconds is done and its effect also to the volume flow rate. The fluid flow rate have inverse relation with pressure, with increase of one of them the other one will decrease. The required volume flow rated of the engine is calculate with the ECM and then the ECM give the desired pressure of the engine to the electrical fuel pump.

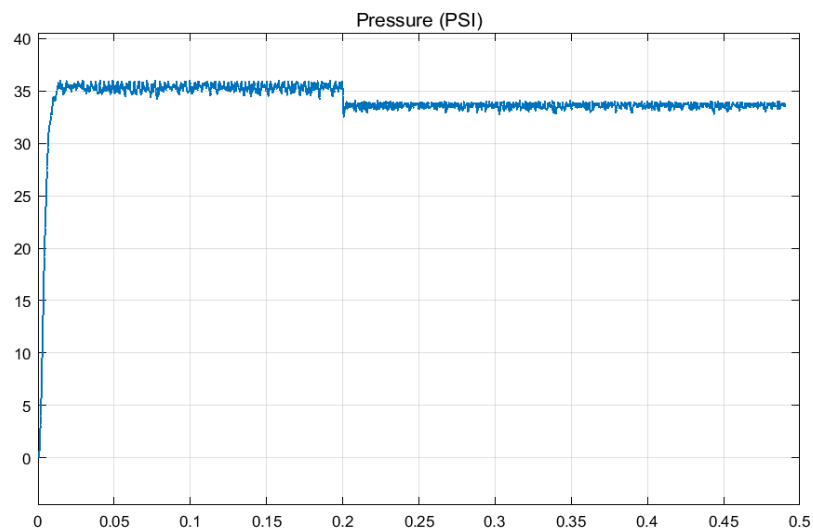


Figure 6.7 Desired pressure change

Hydraulic pressure change has effect on other characteristics of the fluid. In the following figures the pressure change effect on volume flow rate of fluid and torque are shown. In figure 6.8, the volume flow rate of the pump and its performance with respect to the pressure change is shown.

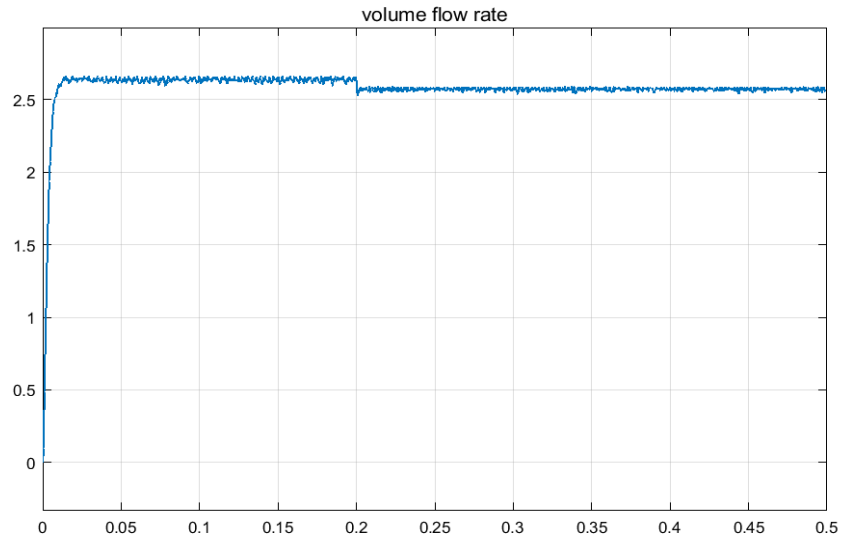


Figure 6.8 Volume flow rate of the pump

The pressure change also have effect on the torque of the motor. In figure 6.9, the torque performance with change of the pressure is shown. As it is shown in the figure, the torque value is decreasing with the decrease of the pump pressure.

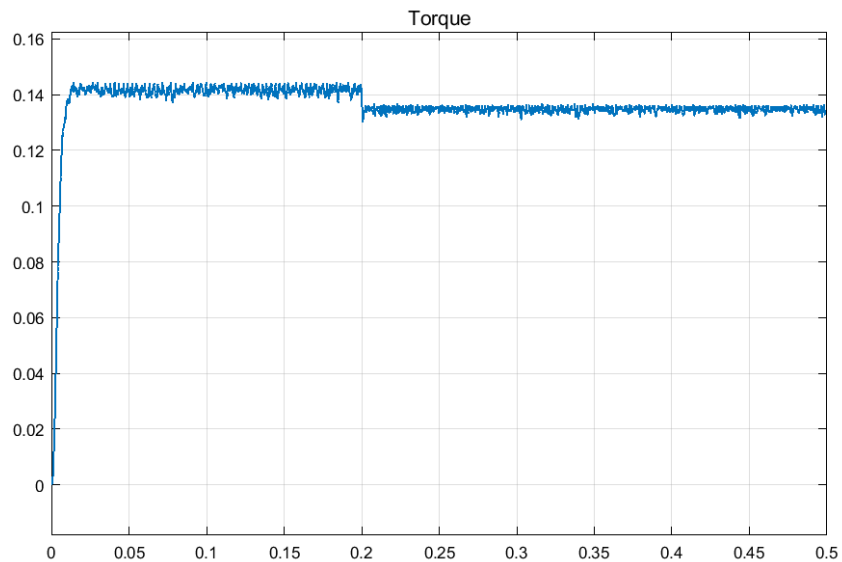


Figure 6.9 Torque of the pump (motor)

And also the pump power is shown in figure 6.10. Due to the decreasing of the shaft rotation speed and also decrease of the torque, power of the pump is also decreasing.

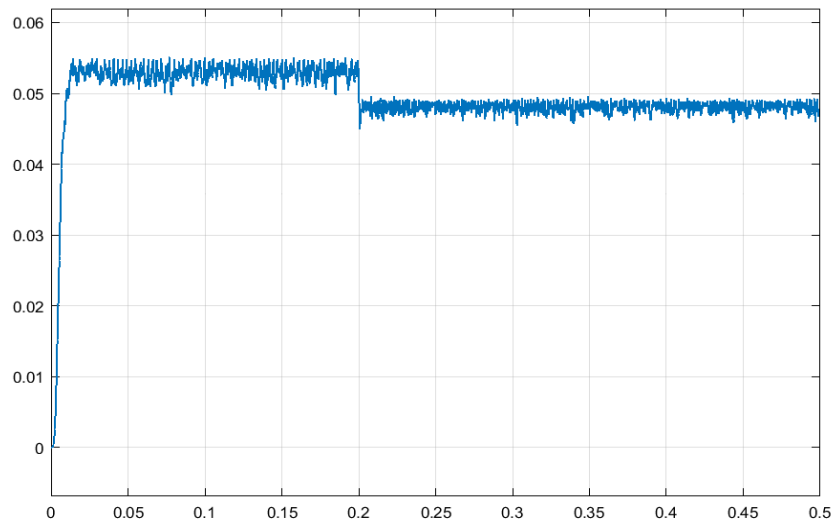


Figure 6.10 Power of the electrical pump

6.3 Battery SOC effect

The battery voltage is changing according to SOC of the battery as it is described in section 5.4, the result of voltage variation has effect on the operation of the pump. The voltage change mainly has effect on the speed of the motor, and then the change of the speed of the motor cause the variation of pressure and other hydraulic and electrical parameters. In figure 6.11, the voltage change of the motor and its effect on the speed of the motor in no-load condition is shown.

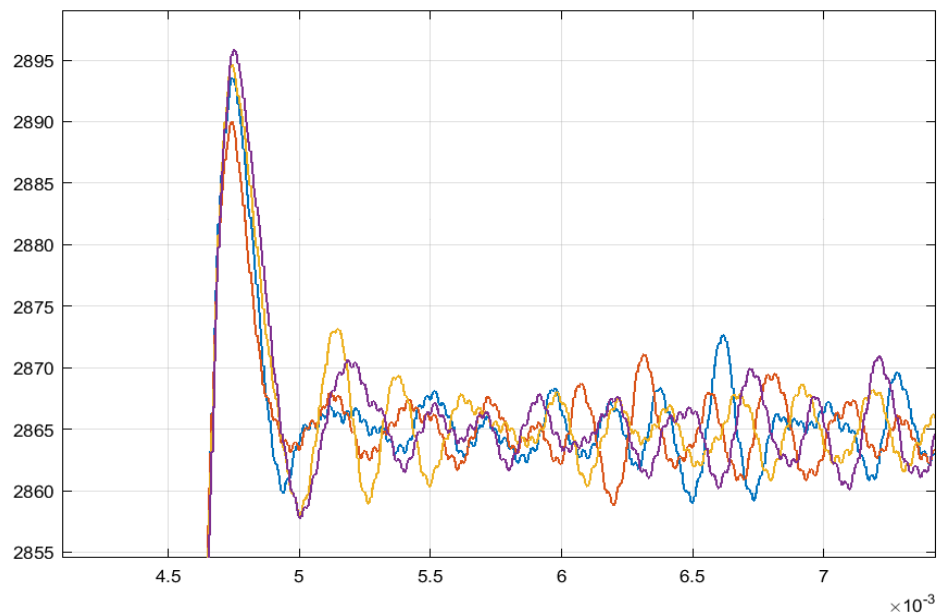


Figure 6.11 SOC effect on speed of the motor

As it shown in the figure 6.11, the voltage decreasing cause speed reduction of the motor. The result is for voltages 12.73 V, 12.50 V, 12.10 V and 11.88 V. The speed difference between the maximum voltage and minimum voltage is 7 rpm.

Also, the effect of the SOC changing in the pump pressure is shown in the figure 6.12. The difference of the pressure for 12.73 V and 11.88 V voltage supply of the motor is almost 0.1 psi.

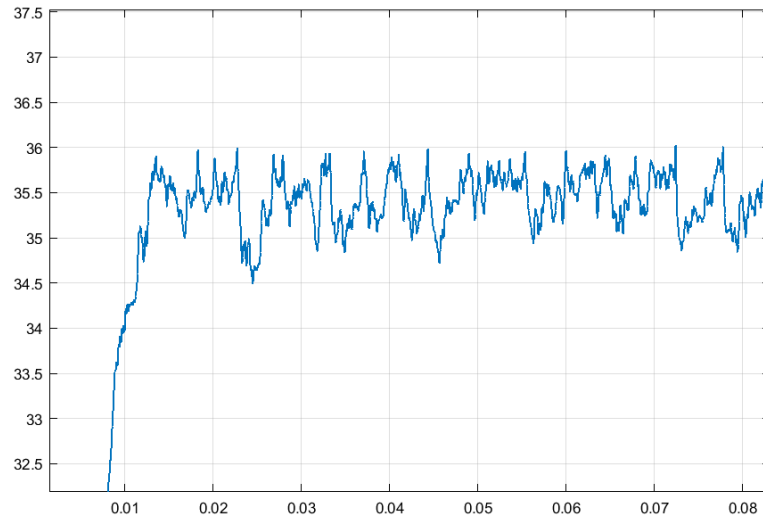


Figure 6.12 Pressure of the pump at 12.73 V

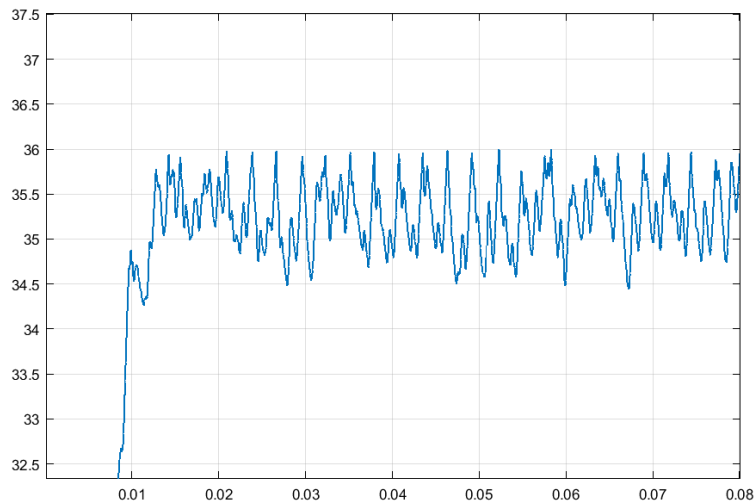


Figure 6.13 Pressure of the pump at 11.88 V

According to the results, the pump delivering the desired pressure. But there are ripples in the pressure of the pump because of the ripples in the motor speed. In summary, the results of the motor and the pumps are acceptable and the pump supply the desired pressure for operation.

Conclusion

The main objective of this thesis is to design field oriented control of brushless (BLDC) motor for controlling hydraulic flow of automotive fuel pump. Motor's characteristic is selected from datasheet of brushless Maxon motor for simulation. Maximum torque per ampere and field oriented control (indirect field oriented control) are designed and implemented into the Matlab and Simulink. MTPA is used to generate directive current that cause creation reluctance torque in the motor. Also, field weakening increase controlling of the motor and when the motor speed goes high that back-emf is equal to the voltage cause reduction of directive current and increasing speed to the desired value.

Regenerative turbine pump is the one of the best pump for supplying high pressure fluid. The hydraulic calculation is done and the simulation the hydraulic part give the desired pressure. The simulation if hydraulic was done in Simscape and pump model in Simscape calculate some friction loss of the pump. The pressure gain of the pump is earn by experimental research of papers.

The pump is designed for automotive and thus the nozzles are used for simulation of fuel pump performance. The nozzles was working like the injection of the fuel in the propulsion system and this cause the result of pump performance become near the real condition of the fuel usage of injected engine of cars.

The results show a good performance of brushless motor and also hydraulic pressure and flow rate. The final pressure of the pump has some ripples but it follow the desired pressure. It is one step forward to delivering the sufficient amount of pressure to the engine.

Due to the time limitation and a expand area of work in motor hydraulic parts the main goal is not fully achieved. In order to fully complete the work, additional work must be consider during the simulation in future.

Some parameters are not taken into consideration because of less time, and in future may be done more in detail for each section hydraulic and motor. The following parameters or condition is not taken into consideration in this thesis.

- Temperature changes in motor that it will change the parameters of motors
- Also temperature change has effect of parameters of hydraulic like's viscosity, Reynold number and some other parameters of fluid.

- The CFD analysis of the pump that give better hydraulic performance result of the pump like hydraulic pressure and losses.
- Finally doing the SIL and HIL testing of the work.

Reference:

1. <https://it.mathworks.com/help/phymod/hydro/ref/fixedisplacementpump.html> [1]
2. Texas Instrument, Teaching Old Motors New Tricks: https://www.youtube.com/watch?v=fpTvZlnrsP0&list=PL15DIIJdJOJ_jPkA-IMgpyS5dXP6NmKY4l&index=1
3. A Study on Advance Electronic Fuel Injection System
4. <https://en.wikipedia.org/wiki>
5. Fuel injection systems (gasoline), Ricardo Pimenta 1050799, Fábio Daniel 1050357
6. Basics on electric motors, EJ Moyer, U. Chicago, April 29, 210
7. Sensorless control of brushless DC motors, PHD thesis submitted to university of Western Sydney, by Markus Tawardas, December 2012
8. A quantitative comparison between BLCD, PMSM, Brushed DC and Stepping motor technology, Stijan Derammelaere, Florian Verbelen, Kurt Stockholm, Department of industrial system and product Design, Gehet University campus Kortijk, Belgium
9. The difference between PMSM & BLDC Motor, Texas Instrument
10. Permanent magnet brushless DC motor drives and controls, Chang-liang Xia Tianjin University, P.R. China, John Wiley & Sons Singapore Pte. Ltd.
11. Brushless DC Motors, Pushek Madaan, Cypress Semiconductor, February 11, 2013
12. Permanent magnet synchronous and brushless DC motor drive, R. Krishnan, 2010, CRC press, ISBN: 978-0-8247-5384-9
13. Comparative analysis of Field oriented control of BLDC motor using SPWM and SVPWM techniques; Pradeep Kumar, Meghana N Gujja; IEEE International Conference On Recent Trends in Electronics Information & Communication Technology (RTEICT), May 19-20, 2017, India
14. Space Vector PWM Intro, <https://www.switchcraft.org/learning/2017/3/15/space-vector-pwm-intro>, May 1, 2017, by [Yngve Solbakken](#)
15. An Improved Design of SVPWM System, Wu Li-hua, Guo Shu-feng, Yang Yang, Deng Shi-jian, 2011 The 6th International Forum on Strategic Technology
16. Performance Analysis of a Permanent Magnet Synchronous Motor Using a Novel SVPWM, Srikanth V, Dr.A Amar Dutt, 2012 IEEE International Conference on Power Electronics, Drives and Energy Systems December 16-19, 2012, Bengaluru, India
17. Perera, P. D. C. (2002). Sensorless Control of Permanent-Magnet Synchronous Motor Drives.
18. Torque Control in Field Weakening Mode, Master Thesis, Group PED4-1038C, 2009, Institute of Energy Technology, Aalborg University
19. Sensorless Control of Brushless DC Motor in Hydraulic Application, Martin Djup, Elias Allar, 2015, Lund university
20. Parameters Identification of a Brushless DC Motor by Specification, Fuad Sh. Al-Mahturi, Dmitry V. Samokhvalov, Vladislav M. Bida, 978-1-5386-4340-2/18/, 2018 IEEE, Saint Petersburg, Russia
21. Comparison and Evaluation of Anti-Windup PI Controllers, Xin-lan Li, Jong-Gyu Park, and Hwi-Beom Shin, Journal of Power Electronics, Vol. 11, No. 1, January 2011
22. Improving Motor Current Control Using Decoupling Technique, Andras Zentai, Tamas Daboczi, Senior Member, IEEE, EUROCON 2005, Serbia & Montenegro, Belgrade, November 22-24, 2005

23. An Optimization Method of the Maximum Torque per Ampere for the Self-tuning of the PMSM Robust, Chi Jie-Fu, Hu Yan-Kui and Zhao Kai, International Journal of Control and Automation, Vol.8, No.11 (2015), pp.69-80
24. FM3 Microcontroller, Field Weakening Control On Wash Machine, Document No. 002-05400 Rev. *B, Cypress Semiconductor Corporation
25. A New Control Technique for Achieving Wide Constant Power Speed Operation with an Interior PM Alternator Machine, Jackson Wai Thomas M. Jahns, 0-7803-7116-X/01/\$10.00 (C) 2001 IEEE
26. Advanced Fuel Pump Technology, Driving Performance And Efficiency, TI Automotive
27. Regenerative Turbine Pumps: The Clear Solution for Volatile Fluids, <http://www.rothpump.com/regenerative-turbine-pumps-volatile-fluids.html>, 24/8/2018, 11:57
28. Quail, Francis J. and Scanlon, T.J. and Baumgartner, A. (2010) Design study of a regenerative pump using one-dimensional and three-dimensional numerical techniques. Numerical Heat Transfer Part A: Applications. ISSN 1040-7782
29. Pump; Contributors: 10elias10, 16@r, 454Casull, A. Balet, A556a, Aatomic1, Abog, Accotink2, Adrian.benko, etc.
30. Rotary vane pump, https://en.wikipedia.org/wiki/Rotary_vane_pump
31. Regenerative turbine pump, <http://www.mthpumps.com/turbine.html>
32. An improved theory for regenerative pump performance, T Meakhail and S O Park, Department of Aerospace Engineering, Korea Advanced Institute of Science and Technology, Taejon, Republic of Korea, DOI: 10.1243/095765005X7565
33. Motor fuel, https://en.wikipedia.org/wiki/Motor_fuel, 02/8/2018
34. Fuel properties, @ 1995-2018 by Isidoro Martinez
35. State of charge, https://en.wikipedia.org/wiki/State_of_charge, 3/08/2018
36. Top 9 Failing Fuel pump symptoms, <http://ricksfreeautorepairadvice.com/fuel-pump-symptoms/>
37. RC Snubbers (SMPS), Illinois Capacitor, INC.
38. Model Based Design: Design with Simulation in Simulink, Ruth-Anne Marchant, @ 2016 MathWorks.
- 39.

Appendix A

MTPA Matlab code

```
% -----MTPA (Maximum Torque Per Ampere Calculation)-----
```

```
clc, clear all, close all,
```

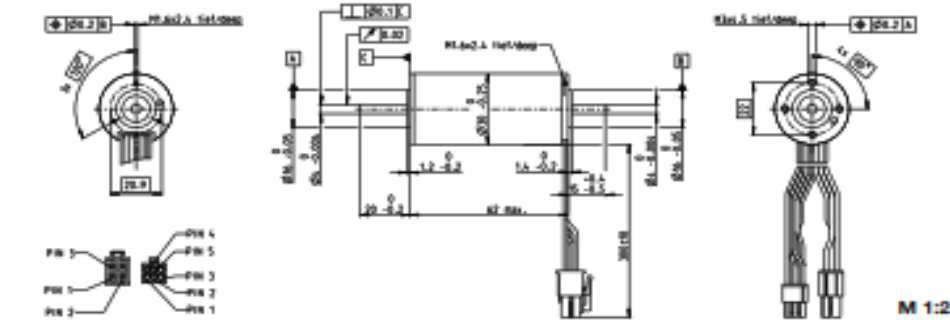
```
Imax=20;           %Maximumallowedcurrent  
p=1;              %NumberofpolesoftheBLDC  
Psim = 0.00946667; %Magneticfluxlinkage  
Lq= 2.45e-05;     %Inductanceinthe q-axis  
Ld= 2.205e-05;   %Inductanceinthe d-axis  
k=1;              %Iterationvariable
```

```
for is=0:Imax/150:Imax  
    poly=[2 Psim/(Ld-Lq) -is*is];  
    R=roots(poly);  
    if(R(1)<R(2))  
        id=R(1);  
    else  
        id=R(2);  
    end  
    iq=sqrt(is*is-id*id);  
    Tm=1.5*p*(Psim+(Ld-Lq)*id)*iq;  
    Vid(k+150)=id;  
    Viq(k+150)=iq;           %Arrayusedinlookup-table  
    VTm(k+150)=Tm;          %Arrayusedinlookup-table  
    if(k>1)  
        Vid(152-k)=-id;  
        Viq(152-k)=-iq;     %Arrayusedinlookup-table  
        VTm(152-k)=-Tm;    %Arrayusedinlookup-table  
    end  
    i=is;  
    k=k+1;  
end
```

Appendix B

Brushless motor Datasheet

EC-max 30 Ø30 mm, brushless, 60 Watt



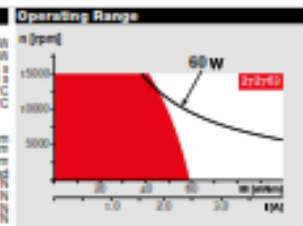
maxon EC-max

Stock program
 Standard program
 Special program (on request)

Part Numbers	23P00	23P05	23P00	23P05
--------------	-------	-------	-------	-------

Motor Data	23P00	23P05	23P00	23P05	
Values at nominal voltage					
1 Nominal voltage	V	12	24	36	48
2 No load speed	rpm	7980	8040	8490	8050
3 No load current	mA	302	191	130	95.4
4 Nominal speed	rpm	6590	8040	8270	8130
5 Nominal torque (max. continuous torque)	mNm	83.6	83.7	83.7	84.1
6 Nominal current (max. continuous current)	A	4.72	2.88	1.88	1.4
7 Stall torque	mNm	381	458	522	519
8 Stall current	A	26.5	18.5	14.5	10.7
9 Max. efficiency	%	80	81	82	82
Characteristics					
10 Terminal resistance phase to phase	Ω	0.447	1.27	2.48	4.49
11 Terminal inductance phase to phase	mH	0.549	0.143	0.312	0.573
12 Torque constant	mNm/A	14.2	34.8	39.9	48.6
13 Speed constant	rpm/V	672	363	266	187
14 Speed/torque gradient	rpm/mNm	21.2	20.6	18.4	18.2
15 Mechanical time constant	ms	4.86	4.73	4.21	4.17
16 Rotor inertia	gcm ²	21.9	21.9	21.9	21.9

- Specifications**
- 17 Thermal data
 - 18 Thermal resistance housing-ambient
 - 19 Thermal resistance winding-housing
 - 20 Thermal (rise constant) winding
 - 21 Thermal time constant motor
 - 22 Ambient temperature
 - 23 Max. winding temperature
 - 24 Mechanical data (preloaded ball bearings)
 - 25 Max. speed
 - 26 Axial play at axial load < 0.0 N
 - 27 Axial play at axial load > 0.0 N
 - 28 Radial play
 - 29 Max. axial load (dynamic)
 - 30 Max. force for press fit (static)
 - 31 Static shaft supported
 - 32 Max. radial load, 5 mm from flange



Comments

- Continuous operation: In observation of above listed thermal resistance (lines 17 and 18) the maximum permissible winding temperature will be reached during continuous operation at 25°C ambient. = Thermal limit.
- Short term operation: The motor may be briefly overloaded (securing).
- Assigned power rating

- Other specifications**
- 33 Number of pole pairs
 - 34 Number of pole pairs
 - 35 Weight of motor
- Values listed in the table are nominal.
- Connection motor (Cable AWG 20)**
- red Motor winding 1 Pin 1
 - black Motor winding 2 Pin 2
 - white Motor winding 3 Pin 3
 - N/C Pin 4
- Connector Pin number**
- Motor 5P-01-3040
- Connection sensors (Cable AWG 20)**
- yellow Hall sensor 1 Pin 1
 - brown Hall sensor 2 Pin 2
 - grey Hall sensor 3 Pin 3
 - blue GND Pin 4
 - green V_{CC} 24 VDC Pin 5
 - N/C Pin 6
- Connector Pin number**
- Motor 40-25-0000
- Wiring diagram for Hall sensors see p. 41

maxon Modular System Overview on page 28–36

- Planetary Gearhead Ø32 mm 1.0 – 8.0 Nm Page 33/34/1
- Maxdrive Ø32 mm 1.0 – 4.5 Nm Page 34/3
- Planetary Gearhead Ø42 mm 3 – 15 Nm Page 34/6

Recommended Electronics: Page 32

- ESCON 36/3 EC 427
- ESCON Mod. 50/4 EC-5 427
- ESCON Module 50/5 427
- ESCON 50/5 428
- DEC Module 50/5 430
- EPOS2 Module 36/2 434
- EPOS2 24/5, 50/5 435
- EPOS2 P 24/5 438
- EPOS4 Module/CE 50/5 442
- MAXPOS 50/5 447

Encoder MR 500/1000 CPT, 3 channels Page 40/4

Encoder HEDL 5540 500 CPT, 3 channels Page 41/7

Brake AS 30 24 VDC 0.1 Nm Page 45/6

October 2017 edition / subject to change